Archive of Applied Mechanics
https://doi.org/10.1007/s00419-024-02540-6

ORIGINAL

Kazuhiro Oda · Shunsuke Ashikari · Nao-Aki Noda

Analysis method useful for calculating various interface stress intensity factors efficiently by using a proportional stress field of a single reference solution modeling

Received: 24 September 2023 / Accepted: 3 January 2024

Abstract This paper has proposed an efficient analysis method to calculate interface stress intensity factors (SIFs) based on a proportional stress field of a reference problem whose exact solution is available. In the previous proportional methods, the same crack length and the same element size were applied to both reference and unknown problems so that the same FEM error can be produced. Therefore, when analyzing many unknown problems, the conventional method needs to analyze many reference problems at the same time. Since this approach is time-consuming, this paper considers how to calculate many crack lengths efficiently by using only one single reference solution modeling. For this purpose, several general relations of SIFs are derived for the unknown and the reference problems when both crack length and element size are different. To analyze many unknown problems accurately by using a single reference solution modeling, how to choose the most suitable element dimension of the reference model is clarified. The proposed method is especially useful for crack propagation analysis.

Keywords Stress intensity factor · Interface crack · Bimaterial plate · Finite element method · Proportional stress field

List of symbols

a	Length of the interface crack in the unknown problem
$2a^*$	Length of the interface crack in the reference problem
C_1, C_2	Normalized factors for short interface edge crack based on the singular stress field at the interface end without the crack
E	Young's modulus
e	Minimum element size at the crack tip in the unknown problem
e^*	Minimum element size at the crack tip in the reference problem

K. Oda (✉)
Division of Mechanical Engineering, Faculty of Science and Technology, Oita University, 700 Dannoharu, Oita-shi, Oita 870-1192, Japan
e-mail: oda-kazuhiro@oita-u.ac.jp

S. Ashikari
Mechanical and Energy Systems Engineering Course, Graduate School of Oita University, 700 Dannoharu, Oita-shi, Oita 870-1192, Japan
e-mail: wizard48695062@gmail.com

N.-A. Noda (✉)
Department of Mechanical Engineering, Kyushu Institute of Technology, 1-1 Sensui-cho, Tobata-ku, Kitakyushu-shi, Fukuoka 804-8550, Japan
e-mail: nao592noda@gmail.com

Published online: 05 March 2024

F_1, F_2	Normalized stress intensity factors for interface crack based on applied stress
G	Shear modulus
H_{11}, H_{22}	Material combination parameters for orthotropic bimaterial
K_1, K_2	Stress intensity factors of an interface crack in the unknown problem
$K_1{}^*, K_2{}^*$	Stress intensity factors of an interface crack in the reference problem
$K_\mathrm{I}, K_\mathrm{II}$	Stress intensity factors of crack in a homogeneous plate
L	Height of the bimaterial plate
r	Distance from the interface crack tip
T, S	Tensile and shear stresses applied to the reference problem
W	Width of the bimaterial plate
α, β	Dundurs' material composite parameters for isotropic bimaterial
$\overline{\alpha}, \overline{\beta}$	Suo's material composite parameters for orthotropic bimaterial
ε	Oscillation singular index of an interface crack
ε_x	Normal strain in x-direction
σ	Applied remote stress
σ_y, τ_{xy}	Stress components along the bimaterial interface
$\sigma_{y,\mathrm{FEM}}(r), \tau_{xy,\mathrm{FEM}}(r)$	Interface stress distributions around the crack for the unknown problem
$\sigma^*_{y,\mathrm{FEM}}(r), \tau^*_{xy,\mathrm{FEM}}(r)$	Interface stress distributions around the crack for the reference problem
$\sigma_{y0,\mathrm{FEM}}, \tau_{xy0,\mathrm{FEM}}$	Stress values at the crack tip node calculated by FEM in the unknown problem
$\sigma^*_{y0,\mathrm{FEM}}, \tau^*_{xy0,\mathrm{FEM}}$	Stress values at the crack tip node calculated by FEM in the reference problem
$\sigma^{T=1*}_{y0,\mathrm{FEM}}, \tau^{T=1*}_{xy0,\mathrm{FEM}}$	Stress values at the crack tip node calculated by FEM in the reference problem under the tensile stress $T = 1$ ($S = 0$)
$\sigma^{S=1*}_{y0,\mathrm{FEM}}, \tau^{S=1*}_{xy0,\mathrm{FEM}}$	Stress values at the crack tip node calculated by FEM in the reference problem under the shear stress $S = 1$ ($T = 0$)
Γ, ρ	Composite parameters representing material anisotropy of orthotropic bimaterial
λ	Order of the stress singularity at the interface end without the crack
ν	Poisson's ratio

1 Introduction

Adhesive joining methods are expanding their use in many industries to reduce weight and improve functionality. When different materials are bonded, a singular stress field is usually generated at the interface end casing interface cracks and leading to final failure. Therefore, it is important to understand the initiation and propagation behavior of interfacial cracks to evaluate the debonding strength of the adhesive joint. Several studies are available regarding interface cracks. Different from ordinary cracks, the interface stress intensity factor SIF varies depending on the material combination as well as the geometries. They are useful for evaluating the interface strength of dissimilar materials [1–8]. Recently, the adhesive strength was discussed in terms of the SIF of the interface crack [9–11]. The authors have shown that the adhesive joint strength can be expressed as a constant value of the intensity of singular stress field (ISSF) at the interface end [12–14]. The authors also have indicated that several joint strengths can be expressed as a constant value of the SIF by assuming a fictitious edge interface crack at the interface end [15, 16]. Those interface fracture mechanics approach shows the usefulness of the solution of the edge interface crack.

Regarding ordinary cracks, Nisitani found that the stress value at the crack tip obtained by the finite element analysis can be a parameter representing the singular stress field around the crack tip. Based on this, they proposed so-called the crack tip stress method that can evaluate the stress intensity factors conveniently and accurately [17–19]. This method provides us under which conditions two stress fields can be equivalent. Assume that FEM analysis with the same mesh size is applied to two different crack problems. If the FEM stress values at the crack tip is the same, the real SIF is also the same. Here, two problems are denoted as follows; one is a reference problem whose exact SIF is known, and the other is an unknown problem whose SIF must be obtained. Then, the unknown SIF can be calculated from only the two stress values without extrapolation. Here, it is important to apply the same element divisions to the two problems.

Regarding interfacial cracks, even under a simple remote tensile stress T, two distinct oscillation singular stress fields cannot be expressed by applying the same approach useful for the ordinary cracks directly. As a reference problem, therefore, the authors proposed that two exact solutions should be used. Specifically, the authors showed that the stress fields of unknown problems can be successfully created by superposing two

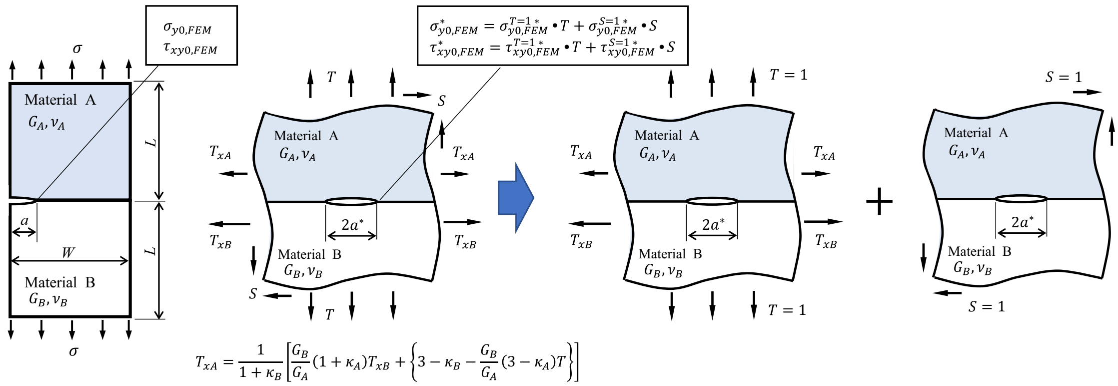

Fig. 1 Illustration how to obtain unknown SIF by adjusting T and S of reference solution to obtain the identical singular stress field **a** An unknown problem and **b** a reference problem consisting of **c**, **d**

fundamental loads, one is by adjusting a remote tensile stress T and the other is by adjusting a remote shear stress S (see Fig. 1) [20–22].

Regarding interfacial cracks, applying the same element size is not enough, and applying the same crack length for the two problems is necessary. This is because the definition of the SIF includes the crack length different from the definition of ordinary cracks. Therefore, when analyzing many unknown problems, it is necessary to analyze many reference problems. In the previous studies, Lan et al. [23] proposed a similar analysis method focusing on the crack open displacement although the element size effect was not examined. Regarding ordinary cracks, Nisitani-Teranishi showed how to calculate SIFs when the element size is not equal although interface cracks were not considered [18, 19]. Considering those situations, this paper will consider how to calculate many different crack lengths efficiently by using only one single reference solution modeling. For this purpose, several useful relations of SIFs will be discussed for the unknown and the reference problems when both crack length and element size are different. Furthermore, to analyze many unknown problems accurately by using a single reference solution modeling, how to choose the most suitable element dimension of the reference model will be clarified. The usefulness will be confirmed for several interface crack problems including an edge crack in orthotropic bimaterial.

2 Conventional proportional method versus new proportional method to calculate SIF

2.1 Conventional proportional method

First, the conventional proportional method will be explained to analyze the interface stress intensity factors [20–22]. In this method, the interface stress intensity factor is calculated by using a proportional stress field of a reference solution. In the method, stress values at the crack tip node are analyzed by applying the finite element method. Then, the stress intensity factor is determined from the crack tip stress values for the unknown problem and the reference problem as shown in Fig. 1. The method provides a proportional singular stress field of the unknown problem in Fig. 1a by adjusting remote tensile stress T and remote shear stress S applied to the reference problem in Fig. 1b whose stress intensity factor is already known. The reference problem in Fig. 1b can be expressed by superposing the problem under tensile stress in Fig. 1c and the problem under shear stress in Fig. 1d.

Figure 2 compares the interface stress distributions around the crack for the unknown problem $\sigma_{y,\mathrm{FEM}}(r)$, $\tau_{xy,\mathrm{FEM}}(r)$ and for the reference problem $\sigma^*_{y,\mathrm{FEM}}(r)$, $\tau^*_{xy,\mathrm{FEM}}(r)$. Figure 2a shows the case when the crack tip normal stress values are matched as $\sigma_{y0,\mathrm{FEM}} = \sigma^*_{y0,\mathrm{FEM}}$ but $\tau_{xy0,\mathrm{FEM}} \neq \tau^*_{xy0,\mathrm{FEM}}$. Figure 2b shows the case when both of the crack tip stress values are matched as $\sigma_{y0,\mathrm{FEM}} = \sigma^*_{y0,\mathrm{FEM}}$ and $\tau_{xy0,\mathrm{FEM}} = \tau^*_{xy0,\mathrm{FEM}}$. The interfacial crack always have peculiar mixed mode singular stress fields due to T and S. However, if both of the crack tip node stress values are matched as $\sigma_{y0,\mathrm{FEM}} = \sigma^*_{y0,\mathrm{FEM}}$ and $\tau_{xy0,\mathrm{FEM}} = \tau^*_{xy0,\mathrm{FEM}}$, the singular stress distributions are the same. Figure 2 shows the FEM stress coincidence, but the real stresses also coincide each other since the same FEM mesh is applied.

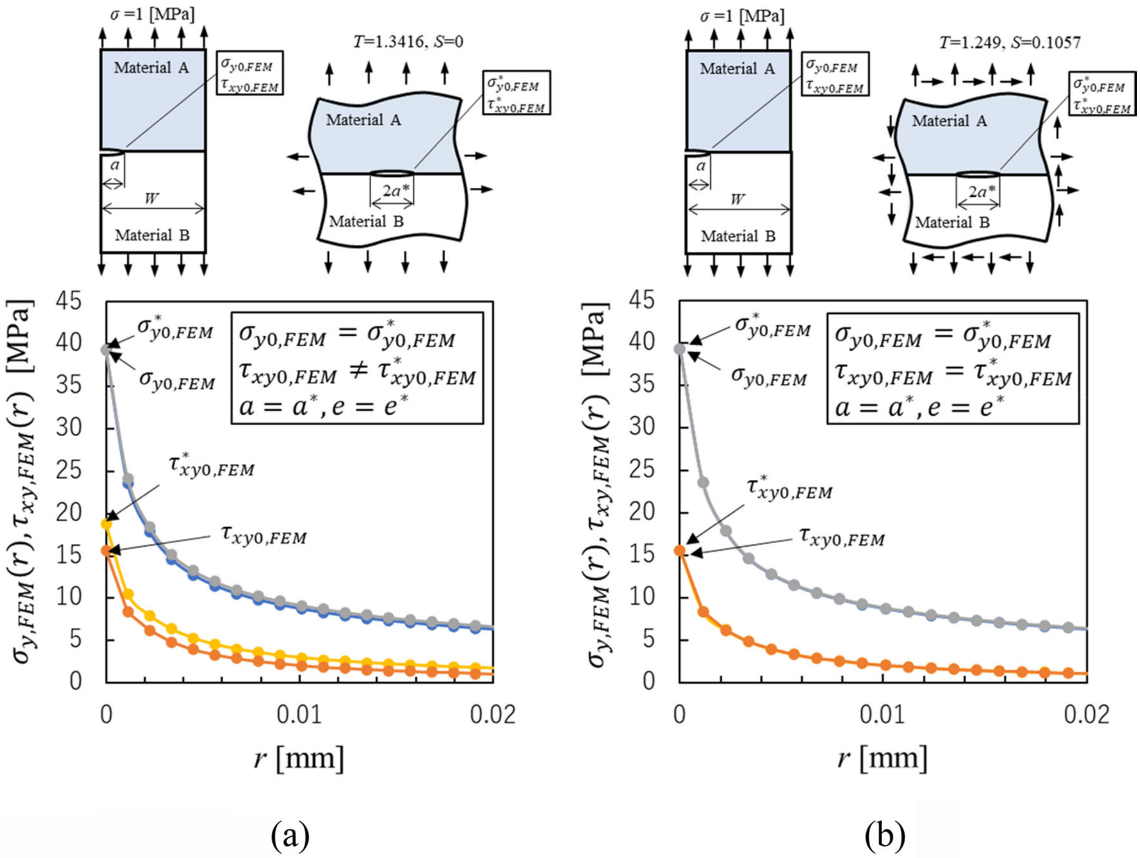

Fig. 2 FEM stress distributions around the interface crack tip for Fig. 1a, b showing that if the FEM crack tip stress is the same as $\sigma_{y0,\,\mathrm{FEM}} = \sigma^*_{y0,\,\mathrm{FEM}}$ and $\tau_{xy0,\,\mathrm{FEM}} = \tau^*_{xy0,\,\mathrm{FEM}}$, the FEM stress distributions are identical. **a** When $\sigma_{y0,\,\mathrm{FEM}} = \sigma^*_{y0,\,\mathrm{FEM}}$ and $\tau_{xy0,\,\mathrm{FEM}} = \tau^*_{xy0,\,\mathrm{FEM}}$ two singular stress fields cannot be identical. **b** When $\sigma_{y0,\,\mathrm{FEM}} = \sigma^*_{y0,\,\mathrm{FEM}}$ and $\tau_{xy0,\,\mathrm{FEM}} = \tau^*_{xy0,\,\mathrm{FEM}}$ two singular stress fields can be identical

The single interface crack in an infinite bimaterial plate subjected to the tension T and shear S in Fig. 1b is selected as the reference problem because the interface crack tip is always mixed mode state. The stress values at the interface crack tip node calculated by FEM in the reference problem under the tensile stress $T = 1$ ($S = 0$) in Fig. 1c are denoted by $\sigma^{T=1*}_{y0,\,\mathrm{FEM}}$, $\tau^{T=1*}_{xy0,\,\mathrm{FEM}}$. The stress values at the interface crack tip node calculated by FEM in the reference problem under the shear stress $S = 1$ ($T = 0$) in Fig. 1d are denoted by and $\sigma^{S=1*}_{y0,\,\mathrm{FEM}}$, $\tau^{S=1*}_{xy0,\,\mathrm{FEM}}$. Also, the crack tip stress values of the unknown problem are also denoted by $\sigma_{y0,\,\mathrm{FEM}}$, $\tau_{xy0,\,\mathrm{FEM}}$. To satisfy the same crack tip stress condition between the reference and the unknown problems, that is, $\sigma_{y0,\,\mathrm{FEM}} = \sigma^*_{y0,\,\mathrm{FEM}}$ and $\tau_{xy0,\,\mathrm{FEM}} = \tau^*_{xy0,\,\mathrm{FEM}}$, the external loading stress T and S in the reference problem can be determined from Eq. (1).

$$T = \frac{\sigma_{y0,\mathrm{FEM}} \cdot \tau^{S=1*}_{xy0,\mathrm{FEM}} - \sigma^{S=1*}_{y0,\mathrm{FEM}} \cdot \tau_{xy0,\mathrm{FEM}}}{\sigma^{T=1*}_{y0,\mathrm{FEM}} \cdot \tau^{S=1*}_{xy0,\mathrm{FEM}} - \sigma^{S=1*}_{y0,\mathrm{FEM}} \cdot \tau^{T=1*}_{xy0,\mathrm{FEM}}},\ S = \frac{\sigma^{T=1*}_{y0,\mathrm{FEM}} \cdot \tau_{xy0,\mathrm{FEM}} - \sigma_{y0,\mathrm{FEM}} \cdot \tau^{T=1*}_{xy0,\mathrm{FEM}}}{\sigma^{T=1*}_{y0,\mathrm{FEM}} \cdot \tau^{S=1*}_{xy0,\mathrm{FEM}} - \sigma^{S=1*}_{y0,\mathrm{FEM}} \cdot \tau^{T=1*}_{xy0,\mathrm{FEM}}}$$
$$\text{when} \quad \sigma_{y0,\mathrm{FEM}} = \sigma^*_{y0,\mathrm{FEM}},\ \tau_{xy0,\mathrm{FEM}} = \tau^*_{xy0,\mathrm{FEM}} \tag{1}$$

The definition of stress intensity factor is based on the interface crack length $2a^*$ as shown in Eq. (2).

$$\sigma_y + i\tau_{xy} = \frac{K_1^* + iK_2^*}{\sqrt{2\pi r}}\left(\frac{r}{2a^*}\right)^{i\varepsilon}, \varepsilon = \frac{1}{2\pi}\ln\left[\left(\frac{\kappa_A}{G_A} + \frac{1}{G_B}\right)/\left(\frac{\kappa_B}{G_B} + \frac{1}{G_A}\right)\right] \tag{2}$$

Here, r is the distance from the crack tip, $2a^*$ is the crack length of the reference problem. The notation ε is the oscillation singular index, shear modulus G_j, $\kappa_j = 3 - 4\nu_j$ (plane strain), $\kappa_j = (3 - \nu_j)/(1 + \nu_j)$ (plane stress) and Poisson's ratio ν_j ($j = A,\ B$). The subscript "j" represents the material A and B. From the

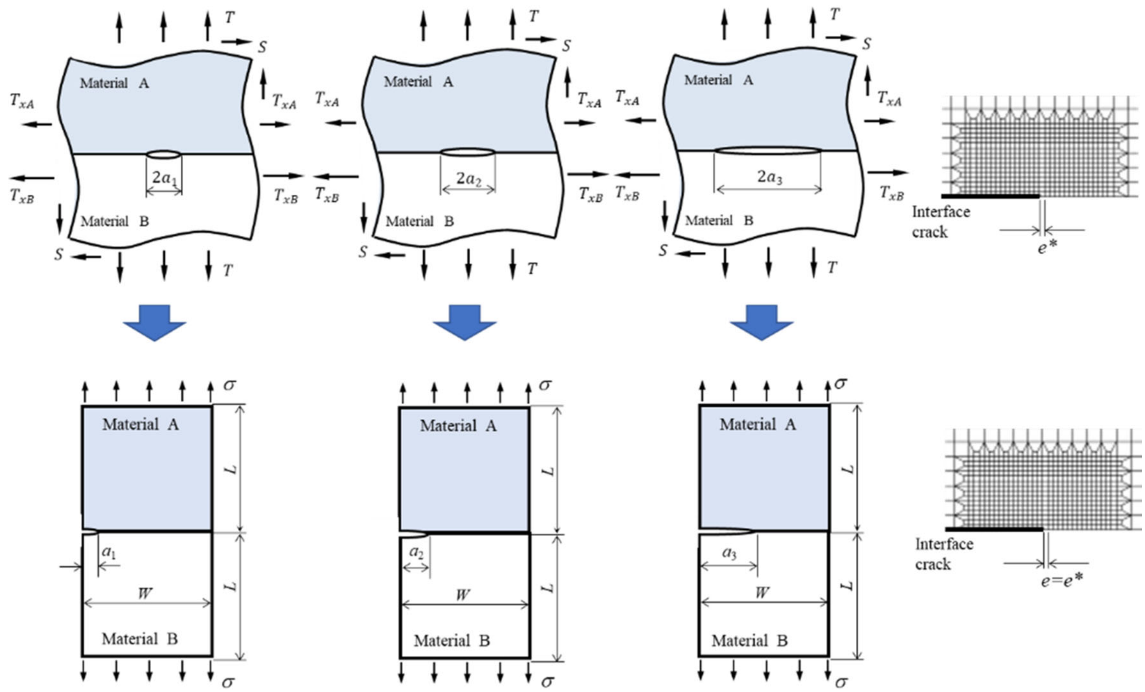

Fig. 3 Conventional proportional method where reference solution models have the same crack length and the same minimum mesh size of the unknown problems as $a^* = a$ and $e^* = e$. If many crack lengths a_1, a_2, a_3.. must be solved for unknown problem, many reference models a_1, a_2, $a_3\ldots$ must be solved

remote stresses T and S obtained by Eq. (1), the interface stress intensity factor of the reference problem can be expressed as

$$K_1^* + iK_2^* = (T + iS)\sqrt{\pi a^*}(1 + 2i\varepsilon), \quad \text{with } T, S \text{ in Eq. (1)}. \tag{3}$$

From $\sigma_{y0,\,\mathrm{FEM}} = \sigma^*_{y0,\,\mathrm{FEM}}$, $\tau_{xy0,\,\mathrm{FEM}} = \tau^*_{xy0,\,\mathrm{FEM}}$, the stress intensity factor of Eq. (3) is equal to that of the unknown problem as shown in Eq. (4).

$$\begin{aligned} &K_1 + iK_2 = K_1^* + iK_2^* = (T + iS)\sqrt{\pi a^*}(1 + 2i\varepsilon), \quad \text{with } T, S \text{ in Eq. (1)} \\ &\text{when } e = e^*,\ a = a^*,\ \sigma_{y0,\mathrm{FEM}} = \sigma^*_{y0,\mathrm{FEM}},\ \tau_{xy0,\mathrm{FEM}} = \tau^*_{xy0,\mathrm{FEM}}. \end{aligned} \tag{4}$$

In the conventional proportional method, the FEM models of the reference and the unknown problems have the same crack length and the same FEM mesh pattern around the interface crack tip. Therefore, the same number of FEM models must be prepared for the reference problems as well as the unknown problems, as indicated in Fig. 3 [20–22].

2.2 New proportional method useful for solving different crack length by using a single reference solution

Figure 4 illustrates interfacial edge crack problems considered in this Section. Assume many different crack lengths a_1, a_2, $a_3\ldots$ must be solved by using only one reference model whose crack length $2a^*$. In the unknown problems, the crack lengths are different $a^* \neq a_k (k = 1, 2, 3\ldots)$, but the FEM element sizes are the same $e = e^*$. At this time, Eqs. (1)~(4) in Sect. 2.1 can be applied, but the crack length difference should be considered for Eqs. (3) and (4). To satisfy the same FEM stress $\sigma_{y0,\,\mathrm{FEM}} = \sigma^*_{y0,\,\mathrm{FEM}}$ and $\tau_{xy0,\,\mathrm{FEM}} = \tau^*_{xy0,\,\mathrm{FEM}}$ at the crack tip for the reference and the unknown problems, the external remote stress T and S in the reference problem can be determined from Eq. (1). Then, the stress intensity factor $K_1 = K_1^*$, $K_2 = K_2^*$ can be determined from Eq. (2). However, it should be noted that $K_1 = K_1^*$, $K_2 = K_2^*$ are defined on the basis of Eq. (3) including the oscillation term $(r/2a^*)^{i\varepsilon}$ regarding the crack length $2a^*$. Generally, the stress intensity

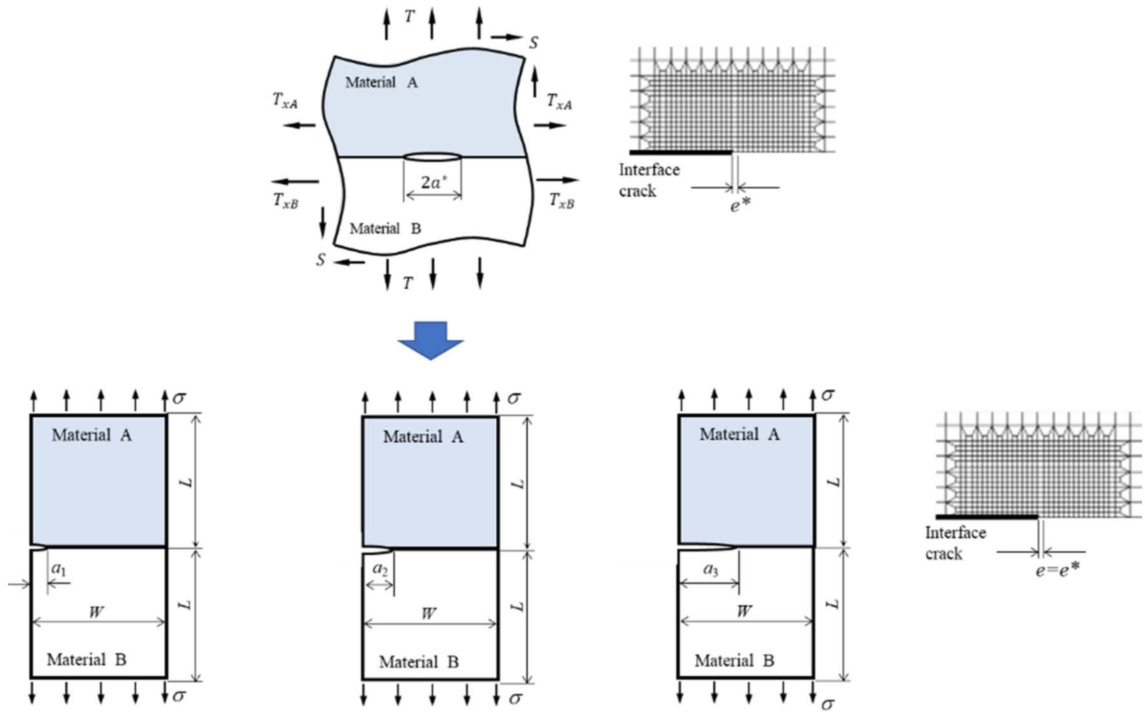

Fig. 4 A new proportional method for calculating the SIF of unknown problems with various crack lengths from a single reference FEM modeling

factor of each interface crack should be expressed from the own crack length $a_k(k = 1, 2, 3 \ldots)$. Therefore, the following equation is applied to converting the stress intensity factor to the own crack length a_k.

$$K_1 + iK_2 = (K_1^* + iK_2^*)\left(\frac{a_k}{a^*}\right)^{i\varepsilon} = (T + iS)\sqrt{\pi a^*}(1 + 2i\varepsilon)\left(\frac{a_k}{a^*}\right)^{i\varepsilon} \quad \text{with } T, S \text{ in Eq. (1)}$$
$$\text{when } e = e^*, a_k \neq a^*,\ \sigma_{y0,\text{FEM}} = \sigma^*_{y0,\text{FEM}},\ \tau_{xy0,\text{FEM}} = \tau^*_{xy0,\text{FEM}}. \tag{5}$$

2.3 New proportional method useful for solving different FEM mesh by using a single reference solution

Next, as shown in Fig. 5, consider several unknown problems whose element size around the crack tip is different by using one reference solution modeling. Regarding an ordinary crack in a homogeneous plate ($G_A = G_B, \nu_A = \nu_B$), Fig. 6 shows the FEM stress distributions (a) $\sigma_{y,\text{FEM}}(r)$ and (b) $\sqrt{e} \cdot \sigma_{y,\text{FEM}}(r/e)$ when $a/W = 0.1$ including the FEM crack tip stress $\sigma_{y0,\text{FEM}}$ by varying the FEM element size around the crack tip. Figure 6 is useful for examining how to apply the reference problem whose mesh size is different from unknown problem. In Fig. 6, the crack length is fixed as $a = 10$ mm and the minimum element dimension at the crack tip varies as $e_1 = a/33 \times 3^{-7}$, $e_2 = a/33 \times 3^{-5}$, $e_3 = a/33 \times 3^{-3}$.

As shown in Fig. 6a, the stress distribution $\sigma_{y,\text{FEM}}(r)$ as well as crack tip stress $\sigma_{y0,\text{FEM}}$ increase with decreasing the minimum element size although the real stress $\sigma_{y0,\text{FEM}}$ becomes infinity. As shown in Fig. 6b, however, the distributions $\sqrt{e} \cdot \sigma_{y,\text{FEM}}(r/e)$ are almost independent of the element dimension e. It may be concluded that the value at the crack tip node stress $\sqrt{e} \cdot \sigma_{y0,\text{FEM}}$ is almost constant when the same problem is analyzed by varying element size e. This is because the FEM stress value at the crack tip node is calculated as the extrapolating value of the stress values at the integration points of the surrounding elements, which is proportional to $1/\sqrt{r}$ [24]. Therefore, when the crack problem of homogeneous material is analyzed by FEM with different element sizes e^* and e, the crack tip stress difference due to element size can be expressed as

$$\sqrt{e} \cdot \sigma_{y0,\text{FEM}} = \sqrt{e^*} \cdot \sigma^*_{y0,\text{FEM}}.$$

The stress distributions are also identical and can be expressed as

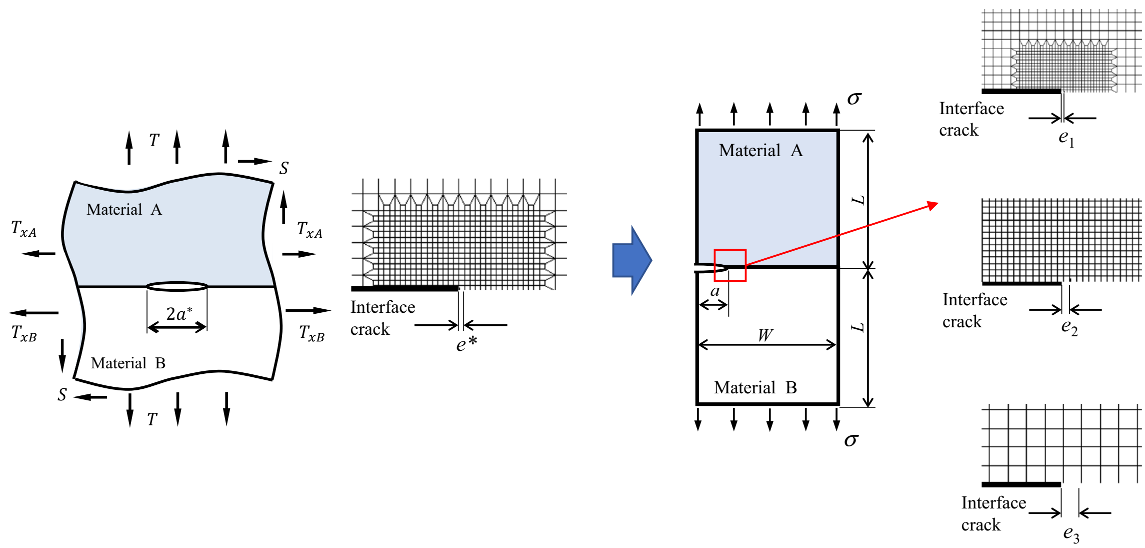

Fig. 5 A new proportional method for calculating the SIF of unknown problem with various mesh sizes from a single reference FEM model

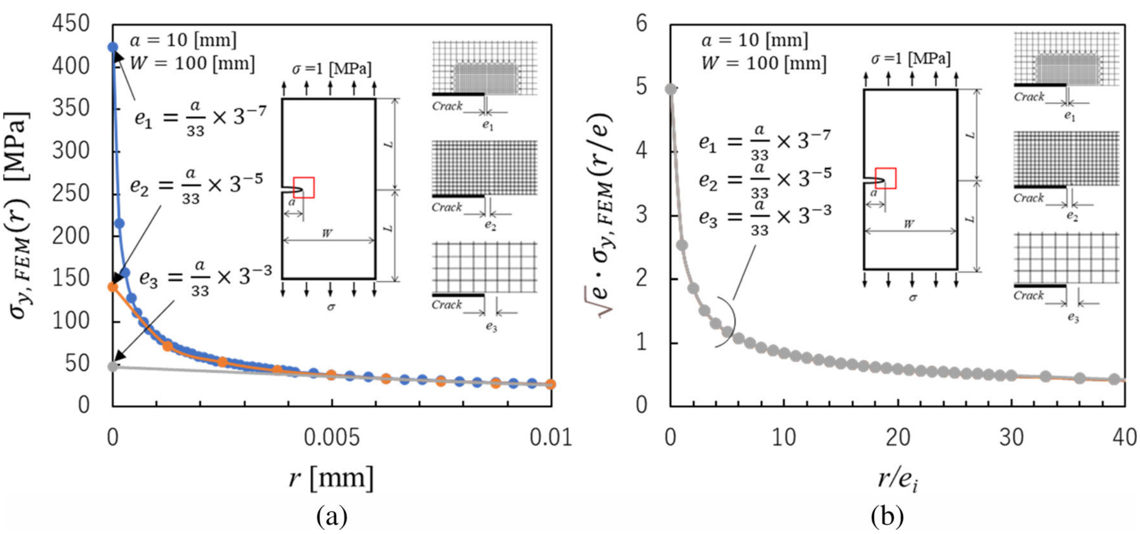

Fig. 6 Mesh dependency of $\sigma_{y,\mathrm{FEM}}(r)$ and mesh-independency of $\sqrt{e} \cdot \sigma_{y,\mathrm{FEM}}(r/e)$ for an edge crack in homogeneous finite plate when $G_A = G_B, \nu_A = \nu_B, a = 10$ mm, $a/W = 0.1$ in Fig. 1a. **a** FEM stress distribution $\sigma_{y,\mathrm{FEM}}(r)$ by varying the element size e_i. **b** $\sqrt{e} \cdot \sigma_{y,\mathrm{FEM}}(r/e)$ is independent of e_i

$$\sqrt{e} \cdot \sigma_{y,\mathrm{FEM}}(r/e) = \sqrt{e^*} \cdot \sigma^*_{y,\mathrm{FEM}}\left(r/e^*\right).$$

Therefore, when the crack problem of homogeneous material is analyzed by FEM with different element sizes e and e^*, their stress intensity factors K_I, K_I^* have a following relation (6) when $\sigma_{y0,\mathrm{FEM}} = \sigma^*_{y0,\mathrm{FEM}}$.

$$K_I = \sqrt{\frac{e}{e^*}} K_I^* = \sqrt{\frac{e}{e^*}} T\sqrt{\pi a^*} \text{ in Fig. 1 with } G_A = G_B,\ \nu_A = \nu_B$$
$$\text{when } e \neq e^*, a = a^*,\ \sigma_{y0,\mathrm{FEM}} = \sigma^*_{y0,\mathrm{FEM}} \tag{6}$$

Equation (6) can be used to determine the SIF of an unknown problem from a SIF of a reference solution. Here,K_I denotes the SIF of the unknown problem $(a,\ W,\ e)$ in a homogeneous cracked plate and K_I^* is the

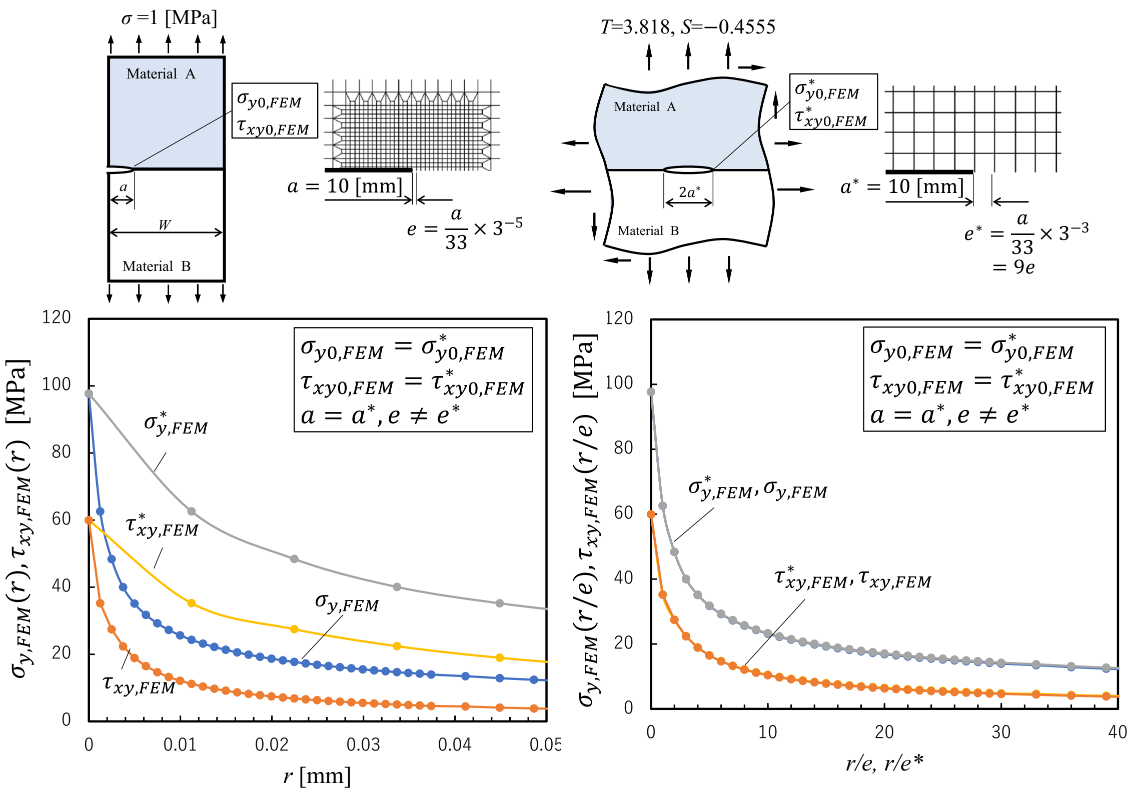

Fig. 7 Effect of the element size on the FEM interface stress distribution for an edge crack in isotropic bimaterial plate when $G_B/G_A = 10$, $\nu_A = \nu_B = 0.3$, $a/W = 0.1$ with $a = 10$ mm, $e = a/33 \times 3^{-5}$, $e = a/33 \times 3^{-5}$ and $e^* = a/33 \times 3^{-3}$. **a** FEM interface stress distributions are not identical since $e \neq e^*$ as $\sigma_{y,\,\mathrm{FEM}}(r) \neq \sigma^*_{y0,\,\mathrm{FEM}}(r)$, $\tau^*_{xy,\,\mathrm{FEM}}(r) \neq \tau^*_{xy,\,\mathrm{FEM}}(r)$ although at the crack tip $\sigma_{y0,\,\mathrm{FEM}} = \sigma^*_{y0,\,\mathrm{FEM}}$, $\tau_{xy0,\,\mathrm{FEM}} = \tau^*_{xy0,\,\mathrm{FEM}}$, **b** FEM interface stress distributions are identical as $\sigma_{y,\,\mathrm{FEM}}(r/e) = \sigma^*_{y,\,\mathrm{FEM}}(r/e^*)$, $\tau_{xy,\,\mathrm{FEM}}(r/e) = \tau^*_{xy,\,\mathrm{FEM}}(r/e^*)$ as well as at the crack tip $\sigma_{y0,\,\mathrm{FEM}} = \sigma^*_{y0,\,\mathrm{FEM}}$, $\tau_{xy0,\,\mathrm{FEM}} = \tau^*_{xy0,\,\mathrm{FEM}}$

SIF of the reference problem (a^*, W^*, e^*) when their FEM stress values at the crack tip are the same as $\sigma^*_{y0,\,\mathrm{FEM}} = \sigma_{y0,\,\mathrm{FEM}}$ under remote tensile stress T.

Due to the oscillation singularity, the effect of the FEM element size of interfacial cracks might be slightly different from the effect of the FEM element size of ordinary cracks. Figure 7a shows the interface stress distribution around the crack tip for the reference and unknown problems with different crack tip element sizes. Here, the crack length is fixed as $a^* = a = 10$mm, the element size for the unknown problem is fixed as $e = a/33 \times 3^{-5}$, and the element size for the reference bimaterial infinite plate is fixed as $e^* = a/33 \times 3^{-3}$. The stress distribution of the unknown problem under remote tensile stress $\sigma = 1$ MPa produces the FEM stress $\sigma_{y0,\,\mathrm{FEM}}$, $\tau_{xy0,\,\mathrm{FEM}}$ at the crack tip. To produce the same FEM stress values as $\sigma_{y0,\,\mathrm{FEM}} = \sigma^*_{y0,\,\mathrm{FEM}}$, $\tau_{xy0,\,\mathrm{FEM}} = \tau^*_{xy0,\,\mathrm{FEM}}$, the remote tensile stress T and the remote shear stress S applied to the reference problem is determined from Eq. (1) as

$$T = 3.73266, \quad S = -0.45552$$

Figure 7a shows that FEM interface stress distributions are not identical as
$\sigma_{y,\,\mathrm{FEM}}(r) \neq \sigma^*_{y,\,\mathrm{FEM}}(r)$, $\tau_{xy,\,\mathrm{FEM}}(r) \neq \tau^*_{xy,\,\mathrm{FEM}}(r)$ although at the crack tip $\sigma_{y0,\,\mathrm{FEM}} = \sigma^*_{y0,\,\mathrm{FEM}}$, $\tau_{xy0,\,\mathrm{FEM}} = \tau^*_{xy0,\,\mathrm{FEM}}$. This is because FEM mesh size is different as $e \neq e^*$. Instead, Fig. 7b shows the stress distributions can be identical when the x-axis is the relative distance r/e as can be expressed as

$$\sigma_{y,\,\mathrm{FEM}}(r/e) = \sigma^*_{y,\,\mathrm{FEM}}\left(r/e^*\right), \; \tau_{xy,\,\mathrm{FEM}}(r/e) = \tau^*_{xy,\,\mathrm{FEM}}\left(r/e^*\right).$$

Regarding interface cracks, therefore, it may be concluded that the SIF of the unknown problems whose element size is different from the element size of the reference problem has the similar relation (6).

When the FEM stress at the interface crack tip is the same for the unknown and the reference problems as $\sigma_{y0,\,\text{FEM}} = \sigma^*_{y0,\,\text{FEM}}$, $\tau_{xy0,\,\text{FEM}} = \tau^*_{xy0,\,\text{FEM}}$ although their crack tip element sizes are different, the following relation can be expected from Fig. 7b and Eq. (2).

$$\frac{K_1 + \mathrm{i}K_2}{\sqrt{2\pi e}}\left(\frac{e}{2a}\right)^{i\varepsilon} = \frac{K_1^* + iK_2^*}{\sqrt{2\pi e^*}}\left(\frac{e^*}{2a^*}\right)^{i\varepsilon} = \sigma_y + i\tau_{xy}\Big|_{r=e} = \sigma_y^* + i\tau_{xy}^*\Big|_{r=e^*}$$
$$\text{when } e \neq e^*,\ a = a^*,\ \sigma_{y0,\text{FEM}} = \sigma^*_{y0,\text{FEM}},\ \tau_{xy0,\text{FEM}} = \tau^*_{xy0,\text{FEM}}. \quad (7)$$

Therefore, Eq. (7) becomes

$$K_1 + iK_2 = \sqrt{\frac{e}{e^*}}(K_1^* + iK_2^*)\left(\frac{e^*}{e}\right)^{i\varepsilon} = \sqrt{\frac{e}{e^*}}(T + iS)\sqrt{\pi a^*}(1 + 2i\varepsilon)\left(\frac{e^*}{e}\right)^{i\varepsilon}$$
$$\text{with } T,\ S \text{ in Eq. (1) when } e \neq e^*,\ a = a^*,\ \sigma_{y0,\text{FEM}} = \sigma^*_{y0,\text{FEM}},\ \tau_{xy0,\text{FEM}} = \tau^*_{xy0,\text{FEM}}. \quad (8)$$

Equation (8) shows the relation of SIF between unknown and reference problems of an isotropic bimaterial whose elastic properties are controlled by $(\alpha,\ \beta)$. Here, K_1, K_2 denote SIFs of an unknown problem $(a,\ W,\ e)$ when the FEM stress value $\sigma_{y0,\,\text{FEM}}$, $\tau_{xy0,\,\text{FEM}}$ appear at the interface crack tip under an external tensile stress. Instead, K_1^*, K_2^* in Eq. (8) denote SIFs of a reference problem $(a^* = a,\ W^*,\ e^*)$ when the same FEM stress $\sigma^*_{y0,\,\text{FEM}} = \sigma_{y0,\,\text{FEM}}$ and $\tau^*_{xy0,\,\text{FEM}} = \tau_{xy0,\,\text{FEM}}$ appear at the interface crack tip under remote stress T, S. Since $T = 3.73266$ and $S =$ -0.45552 are applied to the reference problem as shown in Fig. 7, the SIFs are calculated from Eq. (3) as

$$K_1^* = 3.8181\ \text{MPa}\sqrt{\text{mm}},\ K_2^* = 0.24454\ \text{MPa}\sqrt{\text{mm}}.$$

By substituting $e^*/e = 9$ and $\varepsilon = 0.0093774$ into Eq. (8), the real SIFs for the unknown problem are obtained from Eq. (8) as

$$K_1 = 1.2291\ \text{MPa}\sqrt{\text{mm}} \text{ and } K_2 = 0.3402\ \text{MPa}\sqrt{\text{mm}}.$$

To confirm the accuracy of the new proportional method, by applying the conventional proportional method by using the same element size $e = e^* = a/33 \times 3^{-5}$, the SIFs are calculated as

$$K_1 = 1.2292\ \text{MPa}\sqrt{\text{mm}} \text{ and } K_2 = 0.33999\ \text{MPa}\sqrt{\text{mm}}.$$

The difference between the results of the conventional method and the new method is 0.05% or less, and the Eq. (8) with different element size models gives highly accurate results.

2.4 New proportional method for different crack length and FEM mesh by using a single reference solution

Next, as shown in Fig. 8, let's consider solving several unknown problems whose crack lengths and the element sizes at the crack tip are different by using a single reference problem. As described in Sect. 2.3 and 2.4, when the FEM crack tip stresses are the same as $\sigma_{y0,\,\text{FEM}} = \sigma^*_{y0,\,\text{FEM}}$, $\tau_{xy0,\,\text{FEM}} = \tau^*_{xy0,\,\text{FEM}}$, the relation of SIF between the unknown and the reference problems in an isotropic bimaterial can be expressed as follows from Eqs. (6) and (8).

$$K_1 + iK_2 = \sqrt{\frac{e}{e^*}}(K_1^* + iK_2^*)\left(\frac{e^*}{e}\frac{a}{a^*}\right)^{i\varepsilon} = \sqrt{\frac{e}{e^*}}(T + iS)\sqrt{\pi a^*}(1 + 2i\varepsilon)\left(\frac{e^*}{e}\frac{a}{a^*}\right)^{i\varepsilon},\ \text{with } T, S \text{ in Eq. (1)}$$
$$\text{when } e \neq e^*,\ a \neq a^*,\ \sigma_{y0,\text{FEM}} = \sigma^*_{y0,\text{FEM}},\ \tau_{xy0,\text{FEM}} = \tau^*_{xy0,\text{FEM}} \quad (9)$$

Equation (9) shows the relation of SIF between unknown and reference problems of an isotropic bimaterial whose elastic properties are controlled by $(\alpha,\ \beta)$. Here, K_1, K_2 denote SIFs of an unknown problem $(a,\ W,\ e)$ when the FEM stress value $\sigma_{y0,\,\text{FEM}}$, $\tau_{xy0,\,\text{FEM}}$ appear at the interface crack tip under an external tensile stress. Instead, K_1^*, K_2^* in Eq. (9) denote SIFs of a reference problem $(a^*,\ W^*,\ e^*)$ when the same FEM stress $\sigma^*_{y0,\,\text{FEM}} = \sigma_{y0,\,\text{FEM}}$ and $\tau^*_{xy0,\,\text{FEM}} = \tau_{xy0,\,\text{FEM}}$ appear at the interface crack tip under remote stress T,S.

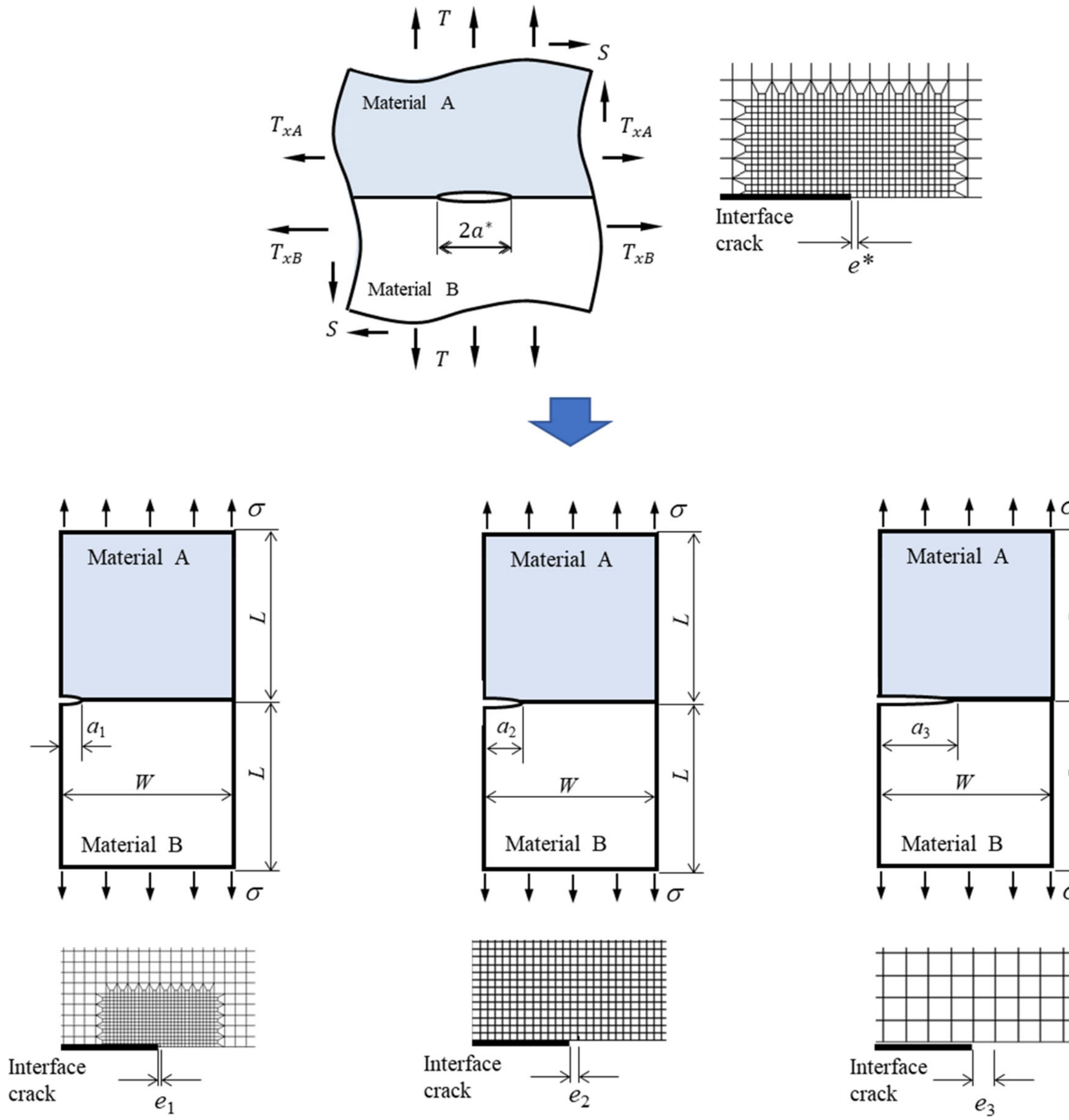

Fig. 8 A new proportional method for calculating the SIF of unknown problems having various crack lengths and different mesh sizes by using a single reference FEM model

If the ratio of the element size to the crack length is the same between the reference and the unknown FEM models is equal as $e^*/a^* = e/a$, the oscillation term becomes $\left(\frac{e^*}{e}\frac{a}{a^*}\right)^{i\varepsilon} = 1$ in Eq. (9). Then, the following relation (10) is obtained.

$$K_1 + iK_2 = \sqrt{\frac{e}{e^*}}(K_1^* + iK_2^*) = \sqrt{\frac{e}{e^*}}(T + iS)\sqrt{\pi a^*}(1 + 2i\varepsilon), \text{ with } T, S \text{ in Eq. (1)}$$

$$\text{when } \frac{e^*}{a^*} = \frac{e}{a}, \left(\frac{e^*}{e}\frac{a}{a^*}\right)^{i\varepsilon} = 1 \text{ but } e \neq e^*,\ a \neq a^*,\ \sigma^*_{y0,\mathrm{FEM}} = \sigma_{y0,\mathrm{FEM}},\ \tau^*_{xy0,\mathrm{FEM}} = \tau_{xy0,\mathrm{FEM}} \quad (10)$$

Equation (10) is a useful SIF relation between the two problems in an isotropic bimaterial whose elastic properties are controlled by (α, β). Here, K_1, K_2 denote SIFs of an unknown problem (a, W, e) when the FEM stress value $\sigma_{y0,\mathrm{FEM}}$, $\tau_{xy0,\mathrm{FEM}}$ appear at the interface crack tip under given external loading. Instead, K_1^*, K_2^* in Eq. (10) denote SIFs of a reference problem (a^*, W^*, e^*) when the same FEM stress appear as $\sigma^*_{y0,\mathrm{FEM}} = \sigma_{y0,\mathrm{FEM}}$, $\tau^*_{xy0,\mathrm{FEM}} = \tau_{xy0,\mathrm{FEM}}$ at the interface crack tip under remote stress T,S.

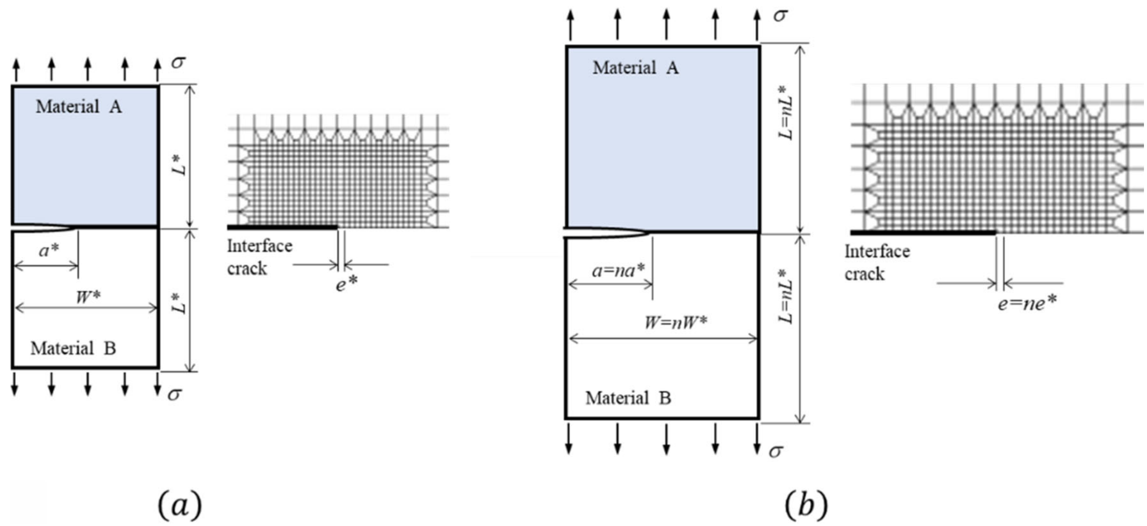

Fig. 9 SIF ratio for the similarity ratio n can be expressed as $\frac{K}{K^*} = \sqrt{\frac{a}{a^*}} = \sqrt{\frac{e}{e^*}} = \sqrt{n}$ under the same remote stress σ and under the similar FEM mesh as $\frac{a}{a^*} = \frac{e}{e^*} = n$. **a** $K^* = K_1^* + iK_2^*$, **b** $K = K_1 + iK_2$

Equation (10) is the same as Eq. (6) for ordinary cracks in a homogeneous plate, which can be also derived by applying the homogeneous material condition $\varepsilon = 0$ to Eq. (9). To understand Eq. (10) intuitively, Fig. 9 illustrates the SIF relation for the interface crack problem having similar dimensions under the same remote stress σ. Assume the similarity ratio n and the FEM mesh is also similar as $a/a^* = e/e^* = n$. Then, the SIF ratio can be expressed as $K/K^* = \sqrt{a/a^*} = \sqrt{e/e^*} = \sqrt{n}$. This is because the dimensionless SIF is the same as $F(a/W) = F(a^*/W^*)$. From $a/a^* = e/e^* = n$, Eq. (10) can also be obtained from Fig. 9.

In the conventional proportional method, it is necessary to apply the same FEM mesh to the reference problem requiring a great deal of labor in creating an FEM model. Instead, this new proportional method has the advantage of being able to efficiently analyze many unknown problems having different crack lengths and element dimensions by using a single reference FEM model.

3 Solution of interface crack SIFs in isotropic bimaterial

In order to confirm the usefulness of the new proportional method explained in Sect. 2, the edge interface crack problem in isotropic bimaterial plate is analyzed as shown in Fig. 1a. The MSC.Marc finite element analysis program is used. The crack length varies from $a = 0.1$ to 10 [mm] corresponding to $a/W = 0.001 \sim 0.1$. The width W and length L of the bonded strip are fixed to $W = 100$ [mm] and $L = 2W$. In Fig. 1a, materials A and B are both isotropic elastic bodies, with shear modulus G_j and Poisson's ratio ν_j (j = A, B). The subscript "j" represents the material A and B. The elastic constants are $G_B/G_A = 10$, $\nu_A = \nu_B = 0.3$ under plane stress condition which were adopted by other researchers [23, 25, 26], the Dundurs composite parameters defined in Eq. (11) are $\alpha = 0.818$, $\beta = 0.286$ and the oscillatory singularity index $\varepsilon = 0.0938$. The tensile stress is set to be $\sigma = 1$ [MPa].

$$\alpha = \frac{G_A(\kappa_B + 1) - G_B(\kappa_A + 1)}{G_A(\kappa_B + 1) + G_B(\kappa_A + 1)}, \beta = \frac{G_A(\kappa_B - 1) - G_B(\kappa_A - 1)}{G_A(\kappa_B + 1) + G_B(\kappa_A + 1)} \tag{11}$$

Table 1 shows the crack tip FEM stress values of the reference problem used in the conventional proportional method when $G_B/G_A = 10$, $\nu_A = \nu_B = 0.3$, $\alpha = 0.818$, $\beta = 0.286$. The minimum element dimension of the reference problem is $e^* = 10/33 \times 3^{-7} = 0.0001386$ [mm], and the plate width is $W^* = 1500a^*$, which can be considered the bonded infinite plate since the plate width independency can be confirmed when $W^* \geq 1500a^*$. In the conventional proportional method, the crack length is set to $a^* = 10, 5, 1, 0.1$ to be equal to the crack length of the unknown problem as $a^* = a$. To analyze four different crack lengths, it is necessary to analyze the corresponding four reference problems as well as four unknown problems. Table 1 can be used as a reference solution's FEM model.

Table 1 An example of FEM stress values at crack tip of reference problem in Fig. 1b used for conventional proportional method by applying the element size $e^* = 10/33 \times 3^{-7}$= 0.0001386 [mm] when $W^* = 1500a^*$, $G_B/G_A = 10$, $\nu_A = \nu_B = 0.3$, $\alpha = 0.818$,$\beta = 0.286$

a^* [mm]	$\sigma_{y0,\mathrm{FEM}}^{T=1*}$ [MPa]	$\tau_{xy0,EFM}^{T=1*}$ [MPa]	$\sigma_{y0,\mathrm{FEM}}^{S=1*}$ [MPa]	$\tau_{xy0,\mathrm{FEM}}^{S=1*}$ [MPa]
10	149.231	– 177.014	317.332	91.316
5	119.867	– 120.713	217.037	72.572
1	67.575	– 48.496	87.988	40.186
0.1	26.826	– 12.265	22.572	15.699

Table 2 shows the obtained SIF of the unknown problem in Fig. 1a when the crack length a= 10, 5, 1, 0.1 [mm], which is corresponding to a/W=0.1, 0.05, 0.01, 0.001 for the fixed geometries $W = 100$[mm], $W^* = 1500a^*$ and for the fixed material combinations $G_B/G_A = 10$, $\nu_A = \nu_B = 0.3$, $\alpha = 0.818$, $\beta = 0.286$. Dimensionless SIFs F_1, F_2 are defined in Eq. (12).

$$F_1 = \frac{K_1}{\sigma\sqrt{\pi a}}, F_2 = \frac{K_2}{\sigma\sqrt{\pi a}} \tag{12}$$

Table 2 explains how much extent F_1, F_2 values in Fig. 1a varies by the unknown problem modeling (a, W, e) and the reference solution modeling (a^*, W^*, e^*). First, at the upper part of Table 2, the results of the conventional method are shown. Second, at the middle part of Table 2, the results of the new method are shown.

Third, at the lower part of Table 2, the results of the new methods recommended are shown. At the upper part of Table 2, the results of the conventional method are obtained by using Eqs. (1), (2), and (4). These results are most reliable since they are obtained by applying the same mesh size and the crack length as $e = e^*$, $a = a^*$ so that the same FEM error can be expected between the unknown and reference problems. The element size is fixed as $e = e^* = 10/33 \times 3^{-7} = 0.0001386$ [mm] for all models.

At the middle part of Table 2, the results of the new proportional method are examined by varying the FEM mesh size as e/e^*=0.1, 3, 10, 100. Here, the reference model is fixed as the crack length a^*= 10 [mm] and the minimum element size $e^* = 10/33 \times 3^{-7}$= 0.0001386 [mm] in Table 1. Since the crack length and the element size are different between the reference problem and the unknown problem, the SIFs are calculated using the relationship in Eq. (9). Compared with the results of the conventional proportional method at the upper part of Table 2, it is seen that the error in F_1 is less than 0.17% and the error in F_2 is less than 1.3%. Even in the new proportional method where both the crack length and the element size are different, the values of F_1 and F_2 is almost the same. It is confirmed that the new proportional method based on Eq. (9) is effective and useful.

At the lower part of Table 2, the results of the new proportional method based on Eq. (10) are shown. The ratio of the element size to the crack length is fixed for the reference and the unknown models as $e^*/a^* = e/a$. Since the ratio $e^*/a^* = e/a$= constant in the reference and the unknown problems, the SIF is calculated by using the Eq. (10). These results are in good agreement to more than four digits with the results of the conventional proposed method. Even though the crack length and the element size are different from the reference problem, it is found that the new proportional method based on relation (10) is very effective and useful. To use the same ratio of the element size to the crack length for the reference and the unknown models as $e^*/a^* = e/a$ is recommended since the same accuracy of the conventional method can be expected although a single reference solution can be applied to different crack length.

Table 3 summarizes F_1, F_2 values for the wide range of $a/W =\rightarrow 0 \sim 0.5$ obtained by the recommended new method based on Eq. (10) in comparison with the results of other researchers when $G_B/G_A = 10$, $\nu_A = \nu_B = 0.3$, $\alpha = 0.818$, $\beta = 0.286$. The present results are in good agreement with the results of Lan et al. obtained by the proportional crack opening displacement method [23]. The absolute values of F_1 and F_2 gradually increase when $a/W \rightarrow 0$ in the range $a/W < 0.1$. The previous papers [27–31] showed that the SIF of a small edge crack is controlled by the singular stress field at the interface end without the crack. As $a/W \rightarrow 0$, one of authors has reported that F_1, F_2 values of the interface edge crack in a bonded strip are controlled by the singular stress field at the interface end without the crack as shown in Eq. (13).

$$F_1 \rightarrow C_1/(a/W)^{1-\lambda},\ F_2 \rightarrow C_2/(a/W)^{1-\lambda} \text{ when } a/W \rightarrow 0 \tag{13}$$

Table 3 shows those C_1, C_2 values defined in Eq. (13) become constant as $a/W \rightarrow 0$ [30]. The values of C_1, C_2 when $a/W \rightarrow 0$ are interpolated by [27, 28]. Here, λ is the singularity index at the interface end when there is no crack.

Table 2 How much extent F_1, F_2 values in an isotropic bimaterial plate in Fig. 1a varies depending on the proportional method modeling for the unknown problem (a, W, e) and the reference solution (a^*, W^*, e^*) under the fixed geometries $W = 100$, $W^* = 1500a^*$ and fixed material combination $G_B/G_A = 10$, $\nu_A = \nu_B = 0.3$, $\alpha = 0.818$, $\beta = 0.286$, (Underline: most reliable value)

Unknown problem to be solved	$a/W = 0.1$ $(a = 10, W = 100)$	$a/W = 0.05$ $(a = 5, W = 100)$	$a/W = 0.01$ $(a = 1, W = 100)$	$a/W = 0.001$ $(a = 0.1, W = 100)$
Conventional method				
By using four reference solution models as $e^* = e$, $a^* = a$	By using a reference solution model when $(a^*, W^*, e^*) = (10, 1500a^*, 1.386 \times 10^{-4})$ as $a/a^* = 1$	By using a reference solution model when $(a^*, W^*, e^*) = (5, 1500a^*, 1.386 \times 10^{-4})$ as $a/a^* = 1$	By using a reference solution model when $(a^*, W^*, e^*) = (1, 1500a^*, 1.386 \times 10^{-4})$ as $a/a^* = 1$	By using a reference solution model when $(a^*, W^*, e^*) = (0.1, 1500a^*, 1.386 \times 10^{-4})$ as $a/a^* = 1$
Underlined SIF denotes most reliable since $e^* = e$, $a^* = a$	F_1 $\underline{1.2290}$, F_2 $\underline{-0.3398}$ when $(a, W, e) = (10, 100, e^*)$	F_1 $\underline{1.2499}$, F_2 $\underline{-0.3613}$ when $(a, W, e) = (5, 100, e^*)$	F_1 $\underline{1.5193}$, F_2 $\underline{-0.4514}$ when $(a, W, e) = (1, 100, e^*)$	F_1 $\underline{2.1728}$, F_2 $\underline{-0.6454}$ when $(a, W, e) = (0.1, 100, e^*)$
New method based on Eq. (9)				
By using a single reference solution model only when $a^* = 10$, $e^* = 1.386 \times 10^{-4}$	By using a single reference solution model when $(a^*, W^*, e^*) = (10, 1500a^*, 1.386 \times 10^{-4})$ then $a/a^* = 1$	By using a single reference solution model when $(a^*, W^*, e^*) = (10, 1500a^*, 1.386 \times 10^{-4})$ then $a/a^* = 0.5$	By using a single reference solution model when $(a^*, W^*, e^*) = (10, 1500a^*, 1.386 \times 10^{-4})$ then $a/a^* = 0.1$	By using a single reference solution model when $(a^*, W^*, e^*) = (10, 1500a^*, 1.386 \times 10^{-4})$ then $a/a^* = 0.01$
Obtained SIF when	F_1, F_2	F_1, F_2	F_1, F_2	F_1, F_2
$e/e^* = 0.1$	1.2282, − 0.3415 when $(a, W, e) = (10, 100, 0.1e^*)$	1.2486, − 0.3628 when $(a, W, e) = (5, 100, 0.1e^*)$	1.5167, − 0.4526 when $(a, W, e) = (1, 100, 0.1e^*)$	2.1694, − 0.6458 when $(a, W, e) = (0.1, 100, 0.1e^*)$
$e/e^* = 1$	1.2290, − 0.3398 when $(a, W, e) = (10, 100, e^*)$	1.2499, − 0.3613 when $(a, W, e) = (5, 100, e^*)$	1.5194, − 0.4512 when $(a, W, e) = (1, 100, e^*)$	2.1733, − 0.6442 when $(a, W, e) = (0.1, 100, e^*)$
$e/e^* = 3$	1.2281, − 0.3396 when $(a, W, e) = (10, 100, 3e^*)$	1.2485, − 0.3614 when $(a, W, e) = (5, 100, 3e^*)$	1.5168, − 0.4522 when $(a, W, e) = (1, 100, 3e^*)$	2.1707, − 0.6476 when $(a, W, e) = (0.1, 100, 3e^*)$
$e/e^* = 10$	1.2270, − 0.3431 when $(a, W, e) = (10, 100, 10e^*)$	1.2477, − 0.3648 when $(a, W, e) = (5, 100, 10e^*)$	1.5164, − 0.4556 when $(a, W, e) = (1, 100, 10e^*)$	2.1709, − 0.6508 when $(a, W, e) = (0.1, 100, 10e^*)$
$e/e^* = 100$	1.2257, − 0.3431 when $(a, W, e) = (10, 100, 100e^*)$	1.2463, − 0.3649 when $(a, W, e) = (5, 100, 100e^*)$	1.5147, − 0.4562 when $(a, W, e) = (1, 100, 100e^*)$	2.1688, − 0.6524 when $(a, W, e) = (0.1, 100, 100e^*)$
Recommended new method based on Eq. (10)				
By using a single reference solution model only when $a^* = 10$, $e^* = 1.386 \times 10^{-4}$	By using a single reference solution model when $(a^*, W^*, e^*) = (10, 1500a^*, 1.386 \times 10^{-4})$ then $a/a^* = 1$	By using a single reference solution model when $(a^*, W^*, e^*) = (10, 1500a^*, 1.386 \times 10^{-4})$ then $a/a^* = 0.5$	By using a single reference solution model when $(a^*, W^*, e^*) = (10, 1500a^*, 1.386 \times 10^{-4})$ then $a/a^* = 0.1$	By using a single reference solution model when $(a^*, W^*, e^*) = (10, 1500a^*, 1.386 \times 10^{-4})$ then $a/a^* = 0.01$
SIF when $a/a^* = e/e^*$ coincides with the most reliable SIF	F_1 $\underline{1.2290}$, F_2 $\underline{-0.3398}$ when $(a, W, e) = (10, 100, e^*)$	F_1 $\underline{1.2499}$, F_2 $\underline{-0.3613}$ when $(a, W, e) = (5, 100, 0.5e^*)$	F_1 $\underline{1.5193}$, F_2 $\underline{-0.4514}$ when $(a, W, e) = (1, 100, 0.1e^*)$	F_1 $\underline{2.1728}$, F_2 $\underline{-0.6454}$ when $(a, W, e) = (0.1, 100, 0.01e^*)$

Table 3 Dimensionless SIFs F_1, F_2 of an edge interface crack in an isotropic bimaterial plate in Fig. 1a when $G_B/G_A = 10$, $\nu_A = \nu_B = 0.3$, $\alpha = 0.818$, $\beta = 0.286$, $\lambda = 0.84081$ (the values C_1, C_2 are indicated in parentheses and the values when $a/W \to 0$ are interpolated by [27, 28])

a/W	F_1				F_2			
	Present (C_1)	Lan [23]	Matsumoto [25]	Miyazaki [26]	Present (C_2)	Lan [23]	Matsumoto [25]	Miyazaki [26]
$\to 0$	$+\infty$ (0.723)	–	–	–	$-\infty$ (− 0.214)	–	–	–
0.001	2.173 (0.724)	–	–	–	− 0.6454 (−0.215)	–	–	–
0.01	1.519 (0.730)	–	–	–	− 0.4514 (−0.217)	–	–	–
0.05	1.245 (0.773)	–	–	–	− 0.3613 (−0.224)	–	–	–
0.1	1.229 (0.852)	1.229	1.222	1.229	− 0.3398 (−0.236)	− 0.340	− 0.336	− 0.340
0.2	1.369 (1.060)	1.369	1.366	1.369	− 0.3496 (−0.271)	− 0.349	− 0.348	− 0.349
0.3	1.648 (1.361)	1.648	1.648	1.648	− 0.3994 (−0.330)	− 0.399	− 0.394	− 0.399
0.4	2.089 (1.805)	2.089	2.090	2.090	− 0.4950 (−0.428)	− 0.495	− 0.491	− 0.494
0.5	2.787 (2.496)	2.787	2.789	2.789	− 0.6634 (−0.594)	− 0.664	− 0.661	− 0.663

4 Solution of interface crack SIFs in orthotropic bimaterial

The interfacial crack analysis method described in Sect. 2 can be applied similarly to the interfacial crack in orthotropic bimaterial. This section explains the stress–strain relationship for orthotropic dissimilar materials, the definition of the stress intensity factor, and how to apply the proportional method.

4.1 Stress–strain relationship and composite parameters of orthogonally anisotropic materials

The relationship between the stress σ and the strain ε of a two-dimensional orthotropic material is given by the following Eq. (14) [32–35].

$$\begin{Bmatrix} \varepsilon_x \\ \varepsilon_y \\ \varepsilon_z \end{Bmatrix} = \begin{bmatrix} \beta_{11} & \beta_{12} & 0 \\ \beta_{21} & \beta_{22} & 0 \\ 0 & 0 & \beta_{66} \end{bmatrix} \begin{Bmatrix} \sigma_x \\ \sigma_y \\ \sigma_z \end{Bmatrix} \tag{14}$$

Under plane stress,

$$\beta_{11} = \frac{1}{E_1}, \beta_{12} = \beta_{21} = -\frac{\nu_{12}}{E_1} = -\frac{\nu_{21}}{E_2}\beta_{22} = \frac{1}{E_2}, \beta_{66} = \frac{1}{G_{12}} \tag{15}$$

Under plane strain,

$$\beta_{11} = \frac{1}{E_1} - \frac{\nu_{31}^2}{E_3}, \beta_{12} = \beta_{21} = -\frac{\nu_{12}}{E_1} - \frac{\nu_{31}\nu_{32}}{E_3}\beta_{22} = \frac{1}{E_2} - \frac{\nu_{32}^2}{E_3}, \beta_{66} = \frac{1}{G_{12}} \tag{16}$$

Here, E_i denotes Young's modulus in the i-direction, G_{12} denotes in-plane shear modulus, and ν_{ij} is the Poisson's ratio expressing shrinkage in the j-direction when the plate is pulled in the i-direction ($i, j = 1, 2$). Assumed that the directions of the two main axes coincide with the x- and y-axes. The following relations holds between each elastic constant.

$$\frac{\nu_{21}}{E_2} = \frac{\nu_{12}}{E_1}, \frac{\nu_{31}}{E_3} = \frac{\nu_{13}}{E_1}, \frac{\nu_{32}}{E_3} = \frac{\nu_{23}}{E_2} \tag{17}$$

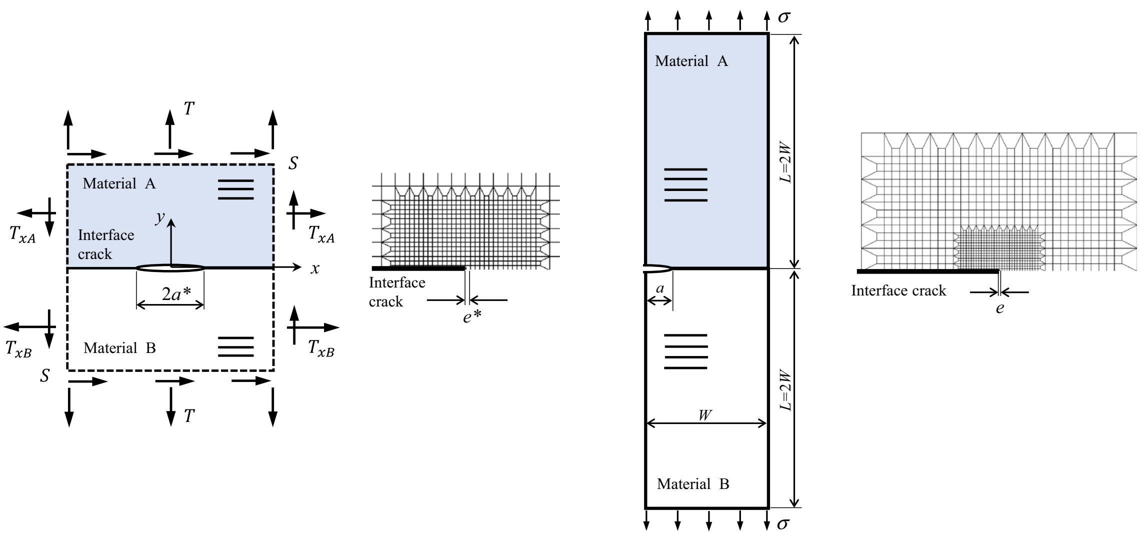

Fig.10 A reference and an unknown interface crack problems in orthotropic bimaterial plate. **a** A center interface crack in orthotropic bimaterial infinite plate ($\varepsilon_{xA} = \varepsilon_{xB}$ at $y = 0$) as a reference problem. **b** An edge interface crack in an orthotropic bimaterial plate as an unknown problem

Suo derives the following $\overline{\alpha}$ and $\overline{\beta}$ corresponding to the Dundurs parameters of an isotropic bimaterial when the main axis of the material coincides with the direction of the interface [32, 33].

$$\overline{\alpha} = \frac{\left\{\sqrt{\beta_{11}\beta_{22}}\right\}_{\mathrm{B}} - \left\{\sqrt{\beta_{11}\beta_{22}}\right\}_{\mathrm{A}}}{\left\{\sqrt{\beta_{11}\beta_{22}}\right\}_{\mathrm{B}} + \left\{\sqrt{\beta_{11}\beta_{22}}\right\}_{\mathrm{A}}}, \overline{\beta} = \frac{\left\{\sqrt{\beta_{11}\beta_{22}} + \beta_{12}\right\}_{\mathrm{B}} - \left\{\sqrt{\beta_{11}\beta_{22}} + \beta_{12}\right\}_{\mathrm{A}}}{\sqrt{H_{11}H_{22}}} \tag{18}$$

$$H_{11} = \left(2n\Gamma^{\frac{1}{4}}\sqrt{\beta_{11}\beta_{22}}\right)_B + \left(2n\Gamma^{\frac{1}{4}}\sqrt{\beta_{11}\beta_{22}}\right)_A, H_{22} = \left(2n\Gamma^{-1/4}\sqrt{\beta_{11}\beta_{22}}\right)_B + \left(2n\Gamma^{-1/4}\sqrt{\beta_{11}\beta_{22}}\right)_A \tag{19}$$

$$\Gamma = \frac{\beta_{11}}{\beta_{22}}, \rho = \frac{2\beta_{12} + \beta_{66}}{2\sqrt{\beta_{11}\beta_{22}}}, n = \sqrt{\frac{1+\rho}{2}} \tag{20}$$

Here, A and B denote Material A and Material B, respectively. In addition, $\overline{\alpha}$ is a parameter representing rigidity, and $\overline{\beta}$ is a parameter related to oscillation singularity of the interface crack.

4.2 New proportional method for the interface crack problem in orthotropic bimaterial

Figure 10a shows the reference problem to be used for analyzing interfacial cracks in the orthotropic bimaterial. Although several definitions have been used for the stress intensity factor for the orthotropic interfacial cracks, in this study, the definition in Eq. (21) proposed by Yuuki et al. will be used [32, 33].

$$\sigma_y + i\sqrt{\frac{H_{11}}{H_{22}}}\tau_{xy} = \frac{K_1 + i\sqrt{\frac{H_{11}}{H_{22}}}K_2}{\sqrt{2\pi r}}\left(\frac{r}{2a^*}\right)^{i\varepsilon} \tag{21}$$

Here, r is the distance from the crack tip, and $2a^*$ is the crack length of the reference problem. The parameters H_{11}, H_{22} in Eq. (21) are defined in Eq. (19). The definition (21) is quite general. When both materials are isotropic but different, by applying the relation $\sqrt{H_{11}/H_{22}} = 1$, the definition (21) coincides with the definition (2) in isotropic bimaterial described in Sect. 2. Also, when both materials are the same isotropic material, by applying the relation $\varepsilon = 0$ the definition (21) coincides with the definition of a homogeneous plate.

Based on this definition, the exact solution of an interface crack in the orthotropic bimaterial infinite plate in Fig. 10a can be expressed in Eq. (22), which is also quite general. When both materials are isotropic but different, by applying the relation $\sqrt{H_{11}/H_{22}} = 1$, the solution (22) coincides with the solution in isotropic dissimilar materials as shown in Eq. (3). Also, when both materials are the same isotropic material, by applying the relation $\varepsilon = 0$ the definition (22) coincides with the exact solution of a crack in a homogeneous infinite plate.

$$K_1^* + i\sqrt{\frac{H_{11}}{H_{22}}}K_2^* = \left\{T + i\sqrt{\frac{H_{11}}{H_{22}}}S\right\}\sqrt{\pi a^*}(1+2i\varepsilon), \quad \text{with } T, S \text{ in Eq. (1)} \tag{22}$$

As described in Sect. 2.4, several unknown problems whose crack lengths and the element sizes at the crack tip are different can be solved by using a single reference problem. When the FEM crack tip stresses are the same as $\sigma_{y0,\,\mathrm{FEM}} = \sigma^*_{y0,\,\mathrm{FEM}}$, $\tau_{xy0,\,\mathrm{FEM}} = \tau_{xy0,\,\mathrm{FEM}}{}^*$, the relation of SIF between the unknown and the reference problems in an orthotropic biomaterial can be expressed as follows:

$$\begin{aligned} K_1 + i\sqrt{\frac{H_{11}}{H_{22}}}K_2 &= \sqrt{\frac{e}{e^*}}\left(K_1^* + i\sqrt{\frac{H_{11}}{H_{22}}}K_2^*\right)\left(\frac{e^*}{e}\frac{a}{a^*}\right)^{i\varepsilon} \\ &= \sqrt{\frac{e}{e^*}}\left(T + i\sqrt{\frac{H_{11}}{H_{22}}}S\right)\sqrt{\pi a^*}(1+2i\varepsilon)\left(\frac{e^*}{e}\frac{a}{a^*}\right)^{i\varepsilon}, \quad \text{with } T, S \text{ in Eq. (1)} \\ &\text{when } e \neq e^*,\ a \neq a^*, \sigma_{y0,\mathrm{FEM}} = \sigma^*_{y0,\mathrm{FEM}},\ \tau_{xy0,\mathrm{FEM}} = \tau^*_{xy0,\mathrm{FEM}} \end{aligned} \tag{23}$$

Equation (23) is the relation of the SIFs for unknown and reference problems in an orthotropic bimaterial whose elastic properties are controlled by $(\overline{\alpha}, \overline{\beta}, \Gamma_A, \Gamma_B, \rho_A, \rho_B)$ defined in Eqs. (18)–(20). Here, K_1, K_2 denote the SIFs of an unknown problem (a, W, e) when the FEM stress value $\sigma_{y0,\,\mathrm{FEM}}$, $\tau_{xy0,\,\mathrm{FEM}}$ appear at the interface crack tip under external loading. Instead, K_1^*, K_2^* in Eq. (23) denote the SIFs of a reference problem (a^*, W^*, e^*) when the same FEM stress value $\sigma_{y0,\,\mathrm{FEM}}$, $\tau_{xy0,\,\mathrm{FEM}}$ appear at the interface crack tip under remote stress T,S. When by applying the isotropic condition $\sqrt{H_{11}/H_{22}} = 1$ to the orthotropic bimaterial, Eq. (23) is reduced to Eq. (9).

To calculate the SIF of the interfacial crack, the ratio of the FEM element size to the crack length can be chosen as $e^*/a^* = e/a$ for the reference and the unknown problems. Under this condition, Eq. (23) becomes Eq. (24).

$$\begin{aligned} K_1 + i\sqrt{\frac{H_{11}}{H_{22}}}K_2 &= \sqrt{\frac{e}{e^*}}\left(K_1^* + i\sqrt{\frac{H_{11}}{H_{22}}}K_2^*\right) = \sqrt{\frac{e}{e^*}}\left(T + i\sqrt{\frac{H_{11}}{H_{22}}}S\right)\sqrt{\pi a^*}(1+2i\varepsilon), \quad \text{with } T, S \text{ in Eq. (1)} \\ \text{when } \frac{e^*}{a^*} &= \frac{e}{a},\ \left(\frac{e^*}{e}\frac{a}{a^*}\right)^{i\varepsilon} = 1 \text{ but } e \neq e^*,\ a \neq a^*,\ \sigma_{y0,\mathrm{FEM}} = \sigma^*_{y0,\mathrm{FEM}},\ \tau_{xy0,\mathrm{FEM}} = \tau^*_{xy0,\mathrm{FEM}} \end{aligned} \tag{24}$$

The relation (24) derived for the orthotropic bimaterial interface crack is the same as the relation (10) for the isotropic bimaterial interface crack and is the same as the relation (6) for the normal crack. This can be explained from the fact that the relation of the SIF having a similar geometrical model in Fig. 9 holds even in the orthotropic bimaterial interface crack problem. Regarding cracks in homogeneous material, the validity of Eq. (6) is explained from the mesh-independency of $\sqrt{e} \cdot \sigma_{y,\,\mathrm{FEM}}(r/e)$ in Fig. 6 in Sect. 2.3. Regarding interface cracks in isotropic bimaterial, the validity of Eq. (10) is explained from the effectiveness of numerical calculation in Table 2 in Sect. 3. Regarding interfacial cracks in orthotropic bimaterial, the validity of Eq. (24) is explained numerically in Table 6 in Sect. 4.2 as follows.

Equation (24) is quite general and includes Eqs. (10) and (6) as special cases. If both materials are isotropic but different, the relation $H_{11}/H_{22} = 1$ can be applied. Then, Eq. (24) coincides with Eq. (10) for isotropic heterogeneous materials discussed in Sect. 2. Also, if both materials are the same isotropic material, the relation $\varepsilon = 0$ can be applied. Then, Eq. (10) coincides with Eq. (6) of a homogeneous plate. Equation (24) is simple and convenient to create FEM meshes effectively when analyzing various stress intensity factors by applying the proportional method.

4.3 Analysis of interfacial crack problem in orthotropic bimaterial

Several interface cracks in orthotropic bimaterial in Fig. 10b are analyzed under plane strain condition by applying the proposed method. Table 4 shows material combinations considered in this study. A material combination AB is a bad pair where the singular stress appears at the interface end [32]. The crack length is

Table 4 An example of material combination of orthotropic bimaterial plate in Fig. 10 [32]

Material combination	E_1 [GPa]	E_2 [GPa]	E_3 [GPa]	G_{12} [GPa]	ν_{12}	ν_{31}	ν_{32}
Bad pair AB							
A	137.9	14.48	14.48	4.98	0.21	0.022	0.21
B	151.7	10.62	10.62	5.58	0.28	0.020	0.28

Material combination	Γ_j	ρ_j	H_{11}	H_{22}	$\overline{\alpha}$	$\overline{\beta}$
Bad pair AB						
A	0.1093	4.515	0.07985	0.2649	0.04422	0.01024
B	0.0755	3.658				

Table 5 An example of FEM stress value at crack tip of the reference problem (a^*, W^*, e^*) in orthotropic bimaterial plate in Fig. 10a which can be used as a reference solution when a^*= 10 [mm], $e^* = 10/33 \times 3^{-7}$=0.0001386 [mm], $W^* = 1500\ a^*$ for the material combination of the bad pair AB in Table 4 where $\Gamma_A = 0.1093$, $\rho_A = 4.515$, $\Gamma_B = 0.0755$, $\rho_B = 3.658$, $\overline{\alpha} = 0.04422$, $\overline{\beta}$=0.01024

a^*[mm]	e^* [mm]	$\sigma^{T=1*}_{y0,\,\mathrm{FEM}}$ [MPa]	$\tau^{T=1*}_{xy0,\,\mathrm{FEM}}$ [MPa]	$\sigma^{S=1*}_{y0,\,\mathrm{FEM}}$ [MPa]	$\tau^{S=1*}_{xy,\,\mathrm{FEM}}$ [MPa]
10	0.0001386	425.241	20.2726	− 9.0482	183.552

set as a= 10 [mm]. Table 5 shows the FEM stress value at the crack tip of the reference solution modeling (a^*, W^*, e^*) when the crack length a^*= 10 [mm], the minimum element size $e^* = 10/33 \times 3^{-7}$=0.0001386 [mm], and the plate width W^*=1500 a^*. Table 5 can be used as a reference solution's FEM model.

Table 6 shows SIFs of an unknown problem. At the upper part, the results of the conventional method are shown by using Eqs. (1) and (22) obtained by using the same crack length and the same element size between the reference problem (a^*, W^*, e^*) and the unknown problems (a, W, e) as $a^* = a$ and $e^* = e$.

Instead, at the middle part in Table 6, the results of the new method are shown obtained from and a single reference solution model under $a^* \neq a$ and $e^* \neq e$. To confirm the validity of Eq. (23), the crack length is changed as a=10~0.1 [mm], and the minimum element size e is changed as $e^*/e = 0.1$, 3, 10, 100 under a fixed reference element size $e^* = 1.3856 \times 10^{-4}$ [mm] and a fixed plate width $W = 100$ [mm]. Regarding the orthotropic interface crack, the difference in F_1 is about 0.3% and the difference in F_2 is about 10%. The difference in F_2 is larger because the absolute value F_2 is small. Compared with the result of the conventional method when $e^*/e = 1$, the difference tends to increase with deviating from $e^*/e = 1$.

At the lower part of Table 6, the results of the new proportional method based on Eq. (24) are shown. The ratio of the element size to the crack length is fixed for the reference and the unknown models as $e^*/a^* = e/a$. Although the ratio e/a=const. in the FEM model, the element size "e" also differs when the crack length "a" differs, so the SIF is calculated using the relationship in Eq. (24). These results are in good agreement to more than four digits with the results of the conventional method where $a^* = a$ and $e^* = e$ are applied. From the above, when using the proportional method, if the FEM model is created so that the ratio e/a is equal between the reference problem and the unknown problem as $e^*/a^*= e/a$, the element size dependence can be almost eliminated, and high accuracy can be achieved. To use the same ratio of the element size to the crack length for the reference and the unknown models as $e^*/a^* = e/a$ is recommended since the same accuracy of the conventional method can be expected although a single reference solution can be applied to different crack length efficiently.

Table 7 shows an example of material constants and composite parameters of orthotropic bimaterial plate in Fig. 10 for bad pair AB [34]. Table 8 shows the dimensionless SIFs of an edge interface crack in orthotropic bimaterial plate for the bad pair AB in the range $a/W = 10^{-2} \sim 10^{-7}$. As shown in Table 8, when $a/W \to 0$, the absolute values of F_1 and F_2 become infinity due to the influence of the interface edge singular field. On the other hand, C_1 and C_2 values are finite and constant when $a/W \to 0$ as clearly indicated in Table 8. In this study, it is found that the values of C_1 and C_2 of a short edge crack in orthotropic bimaterial plate also become constant in the same way of the short edge crack in isotropic bimaterial (see Table 3). It is also confirmed that the recommended new proportional method is useful and efficient to analyze the SIF of extremely short interface cracks.

The interfacial crack in the orthotropic/isotropic bimaterial is also considered. Table 9 shows an example of the material constants and the values of the composite parameters in this analysis. For isotropic material B,

Table 6 How much extent F_1, F_2 values in orthotropic bimaterial plate in Fig. 10b varies depending on the proportional method modeling for the unknown problem $(a,\ W,\ e)$ and the reference solution $(a^*,\ W^*,\ e^*)$ under the fixed geometries $W = 100$, $W^* = 1500a^*$ and the fixed material combination of the bad pair AB in Table 4 where $\Gamma_A = 0.1093$, $\rho_A = 4.515$, $\Gamma_B = 0.0755$, $\rho_B = 3.658$, $\overline{\alpha} = 0.04422$, $\overline{\beta} = 0.01024$ (Underline: most reliable value)

Unknown problem to be solved	$a/W = 0.1$ $(a = 10,\ W = 100)$	$a/W = 0.05$ $(a = 5,\ W = 100)$	$a/W = 0.01$ $(a = 1,\ W = 100)$	$a/W = 0.001$ $(a = 0.1, = W100)$
Conventional method				
By using four reference solution models as $e^* = e$, $a^* = a$	By using a reference solution model when $(a^*,\ W^*,\ e^*) = (10,\ 1500a^*,\ 1.386 \times 10^{-4})$ as $a/a^* = 1$	By using a reference solution model when $(a^*,\ W^*,\ e^*) = (5,\ 1500a^*,\ 1.386 \times 10^{-4})$ as $a/a^* = 1$	By using a reference solution model when $(a^*,\ W^*,\ e^*) = (1,\ 1500a^*,\ 1.386 \times 10^{-4})$ as $a/a^* = 1$	By using a reference solution model when $(a^*,\ W^*,\ e^*) = (0.1,\ 1500a^*,\ 1.386 \times 10^{-4})$ as $a/a^* = 1$
Underlined SIF denotes most reliable since $e^* = e$, $a^* = a$	F_1 $\underline{1.1463}$ F_2 $\underline{-0.0181}$ when $(a,\ W,\ e) = (10,\ 100,\ e^*)$	F_1 $\underline{1.0913}$ F_2 $\underline{-0.0184}$ when $(a,\ W,\ e) = (5,\ 100,\ e^*)$	F_1 $\underline{1.0702}$ F_2 $\underline{-0.0194}$ when $(a,\ W,\ e) = (1,\ 100,\ e^*)$	F_1 $\underline{1.0689}$ F_2 $\underline{-0.0197}$ when $(a,\ W,\ e) = (0.1,\ 100,\ e^*)$
New method based on Eq. (23)				
By using a single reference solution model only when $a^* = 10$, $e^* = 1.386 \times 10^{-4}$	By using a single reference solution model when $(a^*,\ W^*,\ e^*) = (10,\ 1500a^*,\ 1.386 \times 10^{-4})$ then $a/a^* = 1$	By using a single reference solution model when $(a^*,\ W^*,\ e^*) = (10,\ 1500a^*,\ 1.386 \times 10^{-4})$ then $a/a^* = 0.5$	By using a single reference solution model when $(a^*,\ W^*,\ e^*) = (10,\ 1500a^*,\ 1.386 \times 10^{-4})$ then $a/a^* = 0.1$	By using a single reference solution model when $(a^*,\ W^*,\ e^*) = (10,\ 1500a^*,\ 1.386 \times 10^{-4})$ then $a/a^* = 0.01$
Obtained SIF when	F_1 / F_2	F_1 / F_2	F_1 / F_2	F_1 / F_2
$e/e^* = 0.1$	1.1457 / − 0.0191 when $(a,\ W,\ e) = (10,\ 100,\ 0.1e^*)$	1.0910 / − 0.0192 when $(a,\ W,\ e) = (5,\ 100,\ 0.1e^*)$	1.0702 / − 0.0194 when $(a,\ W,\ e) = (1,\ 100,\ 0.1e^*)$	1.0697 / − 0.0198 when $(a,\ W,\ e) = (0.1,\ 100,\ 0.1e^*)$
$e/e^* = 1$	1.1463 / − 0.0181 when $(a,\ W,\ e) = (10,\ 100,\ e^*)$	1.0913 / − 0.0184 when $(a,\ W,\ e) = (5,\ 100,\ e^*)$	1.0702 / − 0.0194 when $(a,\ W,\ e) = (1,\ 100,\ e^*)$	1.0690 / − 0.0198 when $(a,\ W,\ e) = (0.1,\ 100,\ e^*)$
$e/e^* = 3$	1.1436 / − 0.0183 when $(a,\ W,\ e) = (10,\ 100,\ 3e^*)$	1.0887 / − 0.0186 when $(a,\ W,\ e) = (5,\ 100,\ 3e^*)$	1.0676 / − 0.0196 when $(a,\ W,\ e) = (1,\ 100,\ 3e^*)$	1.0664 / − 0.0200 when $(a,\ W,\ e) = (0.1,\ 100,\ 3e^*)$
$e/e^* = 10$	1.1437 / − 0.0201 when $(a,\ W,\ e) = (10,\ 100,\ 10e^*)$	1.0888 / − 0.0203 when $(a,\ W,\ e) = (5,\ 100,\ 10e^*)$	1.0677 / − 0.0212 when $(a,\ W,\ e) = (1,\ 100,\ 10e^*)$	1.0665 / − 0.0216 when $(a,\ W,\ e) = (0.1,\ 100,\ 10e^*)$
$e/e^* = 100$	1.1429 / − 0.0203 when $(a,\ W,\ e) = (10,\ 100,\ 100e^*)$	1.0880 / − 0.0205 when $(a,\ W,\ e) = (5,\ 100,\ 100e^*)$	1.0670 / − 0.0215 when $(a,\ W,\ e) = (1,\ 100,\ 100e^*)$	1.0658 / − 0.0218 when $(a,\ W,\ e) = (0.1,\ 100,\ 100e^*)$
Recommended new method based on Eq. (24)				
By using a single reference solution model only when $a^* = 10$, $e^* = 1.386 \times 10^{-4}$	By using a single reference solution model when $(a^*,\ W^*,\ e^*) = (10,\ 1500a^*,\ 1.386 \times 10^{-4})$ then $a/a^* = 1$	By using a single reference solution model when $(a^*,\ W^*,\ e^*) = (10,\ 1500a^*,\ 1.386 \times 10^{-4})$ then $a/a^* = 0.5$	By using a single reference solution model when $(a^*,\ W^*,\ e^*) = (10,\ 1500a^*,\ 1.386 \times 10^{-4})$ then $a/a^* = 0.1$	By using a single reference solution model when $(a^*,\ W^*,\ e^*) = (10,\ 1500a^*,\ 1.386 \times 10^{-4})$ then $a/a^* = 0.01$
Obtained SIF when $a/a^* = e/e^*$ coincides with the most reliable SIF	F_1 $\underline{1.1463}$ F_2 $\underline{-0.0181}$ when $(a,\ W,\ e) = (10,\ 100,\ e^*)$	F_1 $\underline{1.0913}$ F_2 $\underline{-0.0184}$ when $(a,\ W,\ e) = (5,\ 100,\ 0.5e^*)$	F_1 $\underline{1.0702}$ F_2 $\underline{-0.0194}$ when $(a,\ W,\ e) = (1,\ 100,\ 0.1e^*)$	F_1 $\underline{1.0690}$ F_2 $\underline{-0.0198}$ when $(a,\ W,\ e) = (0.1,\ 100,\ 0.01e^*)$

Table 7 Material constants and combination parameters of orthotropic bimaterial plate in Fig. 10 for bad pair AB [34]

Bad pair AB	E_1 [GPa]	E_2[GPa]	G_{12}[GPa]	ν_{12}	Γ_j	ρ_j	H_{11}	H_{22}	$\overline{\alpha}$	$\overline{\beta}$
Material A	10	40	7.143	0.075	4.00	1.25	3.150	6.075	0.9512	0.3789
Material B	1	0.25	0.1786	0.3	0.25	1.25				

Table 8 SIF an edge interface crack in orthotropic biomaterial plate in Fig. 10b for bad pair AB in Table 7 where $\overline{\alpha} = 0.9512$, $\overline{\beta} = 0.3789$, $\Gamma_A = 4.00$, $\rho_A = 1.25$, $\Gamma_B = 0.25$, $\rho_B = 1.25$, $\lambda = 0.8580$

a/W	F_1	F_2	C_1	C_2
$\to 0$	$\to \infty$	$\to -\infty$	0.766	– 0.335
10^{-7}	7.55	– 3.31	0.766	– 0.335
10^{-6}	5.44	– 2.38	0.766	– 0.335
10^{-5}	3.93	– 1.719	0.766	– 0.335
10^{-4}	2.83	– 1.240	0.766	– 0.335
10^{-3}	2.04	– 0.895	0.766	– 0.336
10^{-2}	1.49	– 0651	0.775	– 0.338

Table 9 Material constants and combination parameters for the orthotropic/isotropic bimaterial plate in Fig. 10

Bad pair	E_1 [GPa]	E_2 [GPa]	G_{12} [GPa]	ν_{12}	Γ_j	ρ_j	H_{11}	H_{22}	$\overline{\alpha}$	$\overline{\beta}$
Material A (orthotropic)	10	40	7.143	0.075	4.00	1.25	0.7869	0.7119	0.7286	0.2113
Material B (isotropic)	3.14	3.14	1.146	0.37	1.00	1.00				

Table 10 SIF an edge interface crack for the orthotropic/isotropic bimaterial plate in Fig. 10b for bad pair AB in Table 9 where $\overline{\alpha} = 0.7286$, $\overline{\beta} = 0.2113$, $\Gamma_A = 4.00$, $\rho_A = 1.25$, $\Gamma_B = 1.00$, $\rho_B = 1.00$, $\lambda = 0.8486$

a/W	F_1	F_2	C_1	C_2
$\to 0$	$\to \infty$	$\to -\infty$	0.786	– 0.197
10^{-7}	9.03	– 2.26	0.786	– 0.197
10^{-6}	6.37	– 1.594	0.786	– 0.197
10^{-5}	4.50	– 1.125	0.786	– 0.197
10^{-4}	3.17	– 0.794	0.786	– 0.197
10^{-3}	2.24	– 0.561	0.786	– 0.197
10^{-2}	1.582	– 0.398	0.788	– 0.198

material parameters $\Gamma_B = \rho_B = 1$. Table 10 shows the dimensionless SIFs, F_1, F_2 defined in Eq. (12), and C_1, C_2 in Eq. (13), respectively. As in Table 10, the absolute values F_1, F_2 become infinity but C_1, C_2 are a finite value when $a/W \to 0$. From Tables 8 and 10, it can be concluded that the recommended proportional method proposed in this study can be also applied to the problem of small interface edge crack in orthotropic bimaterial, and very accurate results can be obtained.

5 Conclusions

Since failures of dissimilar materials often occur near/at the interface, the analysis of interface cracks is important to evaluate the strength. In this study, therefore, a useful analysis method was proposed for the stress intensity factors (SIFs) of interface cracks efficiently by using a proportional stress field of a single reference solution. To analyze an unknown SIF of a given problem, this proportional method uses the FEM results obtained for a reference problem, which is chosen to have the same singular stress field with the exact SIF is available. In the previous studies, the same crack length and the same element size were applied to both reference and unknown problems so that the same FEM error can be produced. Then, by adjusting the external loading so that the same FEM values were obtained, the same SIFs can be expected for the reference and unknown problems. In this approach, therefore, if several number of different crack lengths must be obtained in the unknown problem, the same number of different crack lengths also must be analyzed by the FEM for the reference problem by applying the same mesh pattern. Therefore, this paper studied how to reduce the labor and effort of creating FEM models using the conventional proportional method. As a result, a new proportional method was produced where from the modeling of one reference solution having a crack length with a minimum mesh size, a lot of unknown problems having different crack length can be analyzed. The conclusions can be summarized as follows.

(1) A useful analysis method was proposed for calculating interface stress intensity factors efficiently by using a proportional stress field of a single reference solution whose crack length and whose element size are different from the ones of the unknown problem. In the conventional method, it was necessary to analyze the reference problem having the same crack length and the same element size of the unknown problem, and therefore, when analyzing many unknown problems, it was necessary to analyze the same number of reference problems.

(2) To analyze many unknown problems by using a single reference solution model, the SIF relation (16) between unknown and reference problems in an orthotropic bimaterial was derived when the crack length and the element size are different but the same FEM stress values appear at the interface crack tip. Equation (23) is quite general since it includes the isotropic bimaterial condition (9) and homogeneous plate condition (6).

(3) To analyze many unknown problems accurately by using a single reference solution model, the effect of the element dimension of the reference model was investigated. It was found that the FEM model of the reference problem should be created to satisfy $e^*/a^* = e/a$ since the SIF is almost mesh-independent and most accurate. Here, e^*/a^* is the ratio of the mesh dimension to the crack length of the reference model, and e/a is the one of the unknown models. Under the condition $e^*/a^* = e/a$, the relation (23) is reduced to the relation (24) where the SIF ratio is equal to the root of the ratio of the element dimension as $K_1/K_1^*=K_2/K_2^* = \sqrt{e/e^*}$. Equation (24) for orthotropic bimaterial coincides with Eq. (10) for the isotropic bimaterial and Eq. (6) for homogeneous material, and therefore, Eq. (24) can be used conveniently to create FEM meshes effectively when analyzing various stress intensity factors by applying the proportional method.

(4) Usefulness of the proposed method was verified by analyzing an edge crack in orthotropic bimaterial confirming that the interface stress intensity factors can be calculated efficiently by using a single reference FEM solution. It was shown that the analysis can be performed by the same procedure of the conventional method from the FEM stress to determine the remote stress applied to the reference solution.

(5) It was confirmed that the reference solution of the interface crack of the orthotropic bimaterial is quite general because the solution includes the cases of the isotropic bimaterial and of the isotropic homogeneous material. The proposed method with the single reference solution model can be applied to cracks in orthotropic bimaterials, isotropic bimaterials, and even isotropic homogeneous materials. A general analysis method was proposed for the stress intensity factors (SIFs) of interface cracks efficiently by using a proportional stress field of a single reference solution.

Acknowledgements This work was partially supported by Japan Society for the Promotion of Science, JSPS KAKENHI Grant Number JP 21K03818.

Author contributions K.O. and N.N. wrote the main manuscript text, and S.A. prepared tables 4-10. All authors reviewed the manuscript.

Funding Open Access funding provided by Oita University.

Declarations

Conflict of interest The authors declare no competing interests.

References

1. Erdogan, F.: Stress distribution in bonded dissimilar materials with cracks. J. Appl. Mech. **32**, 403–410 (1965)
2. Rice, J.R.: Elastic fracture mechanics concepts for interfacial cracks. J. Appl. Mech. **55**, 98–103 (1968)
3. Charalambides, P.G., Lund, J., Evans, A.G., McMeeking, R.M.: A test specimen for determining the fracture resistance of bimaterial interfaces. J. Appl. Mech. **56**, 77–82 (1989)
4. O'Dowd, N.P., Shih, C.F., Stout, M.G.: Test geometries for measuring interfacial fracture toughness. Int. J. Solids Struct. **29**, 571–589 (1992)
5. Yuuki, R., Liu, J.-Q., Xu, J.-Q., Ohira, T., Ono, T.: Mixed mode fracture criteria for an interface crack. Eng. Fract. Mech. **47**, 367–377 (1994)
6. Xu, L., Tippur, H.V.: Fracture parameters for interfacial cracks: an experimental-finite element study of crack tip fields and crack initiation toughness. Int. J. Fract. **71**, 345–363 (1995)
7. Chow, W.T., Beom, H.G., Atluri, S.N.: Calculation of stress intensity factors for an interfacial crack between dissimilar anisotropic media, using a hybrid element method and the mutual integral. Comput. Mech. **15**, 546–557 (1995)
8. Ikeda, T., Miyazaki, N., Soda, T.: Mixed mode fracture criterion of interface crack between dissimilar materials. Eng. Fract. Mech. **59**, 725–735 (1998)
9. Afendi, M., Teramoto, T.: Fracture toughness test of epoxy adhesive dissimilar joint with various adhesive thicknesses. J. Solid Mech. Mater. Eng. **4**, 999–1010 (2010)
10. Kinloch, A.J., Shaw, S.J.: The Fracture resistance of a toughened epoxy adhesive. J. Adhesion **12**, 59–77 (1981)
11. Akisanya, A.R., Fleck, N.A.: Interfacial cracking from the free-edge of long bi-material strip. Int. J. Solids Struct. **34**, 1645–1665 (1997)
12. Zhang Y., Wu P., Duan M.: A mesh-independent technique to evaluate stress singularities in adhesive joints. Int. J Adhes. Adhes. **57**, 105–117 (2015), [Zhang Y., Noda, N.-A., Wu P., Duan M.: Corrigendum to "A mesh-independent technique to evaluate stress singularities in adhesive joints. Int. J. Adhes. **60**, 130 (2015)].
13. Miyazaki, T., Noda, N.-A., Ren, F., Wang, Z., Sano, Y., Iida, K.: Analysis of intensity of singular stress field for bonded cylinder and bonded pipe in comparison with bonded plate. Int. J. Adhes. Adhes. **77**, 118–137 (2017)
14. Li, R., Noda, N.-A., Takaki, R., Sano, Y., Takase, Y., Miyazaki, T.: Most suitable evaluation method for adhesive strength to minimize bend effect in lap joints in terms of the intensity of singular stress field. Int. J. Adhes. Adhes. **86**, 45–58 (2018)
15. Noda, N.-A., Miyazaki, T., Uchikoba, T., Li, R., Sano, Y., Takase, Y.: Convenient debonding strength evaluation based on the intensity of singular stress for adhesive joints. J. Japan Inst. Electr. Pack. **17**, 132–142 (2014). (**in Japanese**)
16. Noda, N.-A., Miyazaki, T., Li, R., Uchikoba, T., Sano, Y., Takase, Y.: Debonding strength evaluation in terms of the intensity of singular stress at the interface corner with and without fictitious crack. Int. J. Adhes. Adhes. **61**, 46–64 (2015)
17. Nisitani, H., Kawamura, T., Fujisaki, W., Fukuda, T.: Determination of highly accurate values of stress intensity factor or stress concentration factor of plate specimen by FEM. Japan Soc. Mech. Eng. Series A. **65**(629), 26–31 (1999). ((**in Japanese**))
18. Nisitani, H., Teranishi, T.: Highly accurate values of K_I and K_II of axially symmetrical cracked body subjected to tension obtained by FEM. In: Brebbia, C.A., Selvadurai, A.P.S. (eds.) Damage & Fracture Mechanics VI, vol. 71, pp. 461–469. WIT Press, Amsterdam (2000)
19. Nisitani, H., Teranishi, T.: K_I of a circumferential crack emanating from an ellipsoidal cavity obtained by the crack tip stress method in FEM. Eng. Fract. Mech. **71**, 579–585 (2004)
20. Oda, K., Kamisugi, K., Noda, N.-A.: Analysis of stress intensity factor for interface cracks based on proportional method. Trans. Jpn. Soc. Mech. Eng. Ser. A **75**, 476–482 (2009). (**in Japanese**)
21. Oda, K., Noda, N.-A., Atluri, S.N.: Accurate determination of stress intensity factor for interface crack by finite element method. Key Eng. Mater. **353–358**, 3124–3127 (2007)
22. Kakuno, H., Oda, K., Morisaki, T.: Analysis of stress intensity factor for interfacial crack in bonded dissimilar plate under bending. Key Eng. Mater. **417–418**, 153–156 (2010)
23. Lan, X., Ji, S., Noda, N.-A., Cheng, Y.: Stress intensity factor solutions for several crack problems using the proportional crack opening displacements. Eng. Fract. Mech. **171**, 35–49 (2017)
24. MSC.MARC2012 Manual, Volume A: Theory and User Information, vol 743. MSC. Softwere Corporation (2012)
25. Matsumto, T., Tanaka, M., Obara, R.: Computation of stress intensity factors of interface cracks based on interaction energy release rates and BEM sensitivity analysis. Eng. Fract. Mech. **65**, 683–702 (2000)
26. Miyazaki, N., Ikeda, T., Soda, T., Munakata, T.: Stress intensity factor analysis of interface crack using boundary element method-application of contour integral method. Eng. Fract. Mech. **45**, 599–610 (1993)
27. Noda, N.-A., Lan, X., Michinaka, K., Zhang, Y., Oda, K.: Stress intensity factor of an edge interface crack in a bonded semi-infinite plate. Trans. Jpn. Soc. Mech. Eng. Ser. A **76**, 1270–1277 (2010). (**in Japanese**)
28. Lan, X., Noda, N.-A., Michinaka, K., Zhang, Y.: The effect of material combinations and relative crack size to the stress intensity factors at the crack tip of a bi-material bonded strip. Eng. Fract. Mech. **78**, 2572–2584 (2011)
29. Oda, K., Lan, X., Noda, N.-A., Michinaka, K.: Effect of arbitrary bi-material combination and bending loading conditions on stress intensity factors of an edge interface crack. Int. J. Struct. Integrity **3**, 457–475 (2012)
30. Noda, N.-A., Lan, X.: Stress intensity factors for an edge interface crack in a bonded semi-infinite plate for arbitrary material combination. Int. J. Solids Struct. **49**, 1241–1251 (2012)
31. Oda, K., Takahata, Y., Kasamura, Y., Noda, N.-A.: Stress intensity factor solution for edge interface crack based on the crack tip stress without the crack. Eng. Fract. Mech. **219**, 106612 (2019)

32. Yuuki, R., Xu, J.: Stress intensity factors for the interface crack between dissimilar orthotopic materials. Trans. Jpn. Soc. Mech. Eng. Ser. A **57**, 1542–1549 (1991). (**in Japanese**)
33. Suo, Z.: Singularities, interfaces and cracks in dissimilar anisotorpic media. Proc. R. Soc. Lond. A **427**, 331–358 (1990)
34. Ioka, S., Kubo, S.: Free-edge stress singularity of bonded dissimilar orthotropic materials and its disappearance. Trans. Jpn. Soc. Mech. Eng. Ser. A **70**, 1667–1674 (2004). (**in Japanese**)
35. Beom, H.G., Atluri, S.N.: Dependence of stress on elastic constants in an anisotropic bimaterial under plane deformation; and the interface crack. Comput. Mech. **16**, 106–113 (1995)